POLITECNICO DI MILANO

Facolta di Ingegneria dei Processi Industriali

Dipartimento di Chimica, Materiali e Ingegneria Chimica "Giulio Natta"

STATE OF THE ACT ON ELECTROCHEMICAL SYNTHESIS OF RESISTIVE SWITCHING MATERIALS FOR ReRAM

Relatore: Prof. Silva Franze.

Correlatore: Ing.Dianele Perego

Student:

Anosike Chibueze Francis.

Mat no. 753014.

A.A. 2011/2012

Acknowledgement

It has really been a great pleasure to work with my supervisor Prof. Franz Silvia, she has really been of immense benefit to me in the ways of technical thinking and problem solving and more especially in the diligent ways she answers and attends to my challenges, I thank her so much. I am also thankful to my co-supervisor, Perego Daniele for all his assistance and direction.

I extend my gratitude to all the professors who were so diligent in imparting their knowledge during the course of my program. I also remain grateful to all my friends in Politecnico di Milano that supported me in one way or the other.

My deepest gratitude goes to my parents who have seen to it that I reached this level in life, my lovely wife Mrs. Deborah Ifeoma Anosike for her love and unrelentless support during the most difficult part of the program, I really appreciate her. I completely dedicate this work to my newly born baby boy Obinna Trust Anosike, for the joy, blessing and happiness he has brought to us during the course of this work.

Finally, the highest thanks and appreciation goes to the creator of the entire universe and the whole things in them, the Almight God; Jehovah for the gift of life and making it possible for me to come to the conclusion of this program.

Abbreviation

AAO: Anodized Aluminium Oxide

XRD: X – Ray Diffractometer

EDS: Energy Dispersive Spectroscopy

DC: Direct Current

Cmos: Complementry Metal Oxide Semi Conductor

TMOs: Transition Metal Oxides

MOM : Metal-Oxide-Metal

HRS/LRS: High Resistance and Low Resistance State.

CBRAM : Conductive Bridging Ram

SAEDPS: Selected-Area Electron Diffraction Patterns

Table of Contents

List of Figures

Figure 15.0: (a-d) Morphological observations and EDX analysis of nanostructured ZnO on Ni nanowires with different magnifications. Electrodeposition of Ni from NisNH2SO3d2•4H2O + boric acid at −20 mA/cm2 for 60 min. ZnO electrodeposition in 0.1 M ZnsNO3d2 with application of −1.0 V at 70°C for 60 min**.**

Figure 16.0: X-ray diffraction patterns of (a) ITO (as reference) and TiO2 films deposited by (b) chemical and (c) electrochemical methods on ITO substrate followed by annealing at 500 °C for 1 h in air

Figure 17.0: Insert shows TEM image of the TiO2 film deposited by chemical method followed by annealing at 500 °C for 1 h in air. (b)A high-resolution image of a portion of the investigated image in (a). Results obtained after Fourier transformation of the high-resolution image is as shown in (c)

Figure 18.0: Insert shows TEM image of the TiO2 film deposited by electrochemical method followed by annealing at 500 °C for 1 h in air. (b) A high-resolution image of a portion of the investigated image in (a). Results obtained after Fourier transformation of the high resolution image is as shown in (c).

Figure 19.0: X-ray diffraction patterns of Electrochemically deposited TiO2 thin films annealed at 500 °C for 1 h in air on (a) the glass substrate (b) the quartz substrate and (c) the collected byproduct annealed at 500 °C for 1 h in air

Figure 20.0: SEM images of the TiO2 films deposited by (a) chemical and (b) electrochemical methods followed by annealing at 500 °C for 1 h in air. Inset is the cross-section images, shows the compactness of the films.

Figure 21.0: Surface view AFM image of the TiO2 films deposited by (a) chemical method and (b) electrochemical method followed by annealing at 500 °C for 1 h in air.

1.0 Introduction

High level or rapid advance in information technology rely on high-speed and large-capacity nonvolatile memories. Based on this, a lot of alternatives to contemporary flash memory have been extensively studied to obtain a more powerful and functional nonvolatile memory. But my consideration will focus on current status of one of the alternatives resistive switching phenomena found in transition metal oxide. Therefore, a ReRAM memory cell is a capacitor-like structure composed of insulating or semi conducting transition metal oxides that exhibits reversible resistive switching on applying voltage pulses. It can also be referred to as a new non volatile kind of memories based on idea that dielectric, which is normally insulating, can be made to conduct through a filament or conducting path formed after application of sufficiently high.

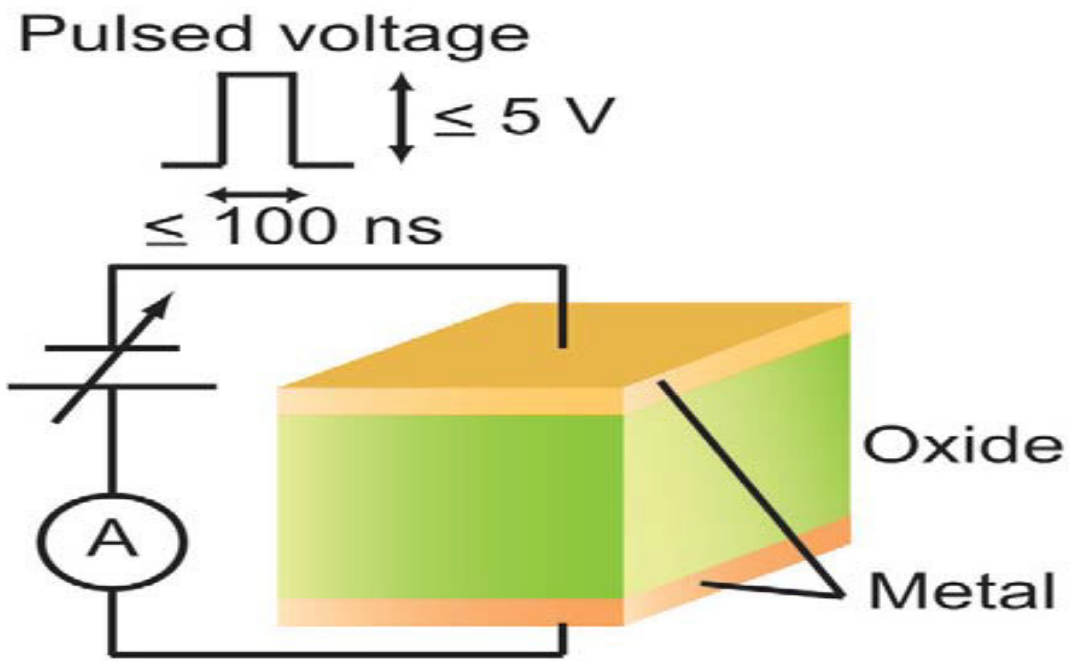

Figure.1: Diagram of ReRAM memory cell with a capacitor-like structure in which an insulating or semi conducting oxide is sand switched between two metal electrode

The major feature of the resistive switching in metal oxide is the ability to switch between a high resistance state and a low resistance state simply by applying pulse voltages. Usually ReRAM metal oxide base, require a preliminary electroforming process called forming. In order to electrically break-up the insulator layer and make conductive the oxide layer. After the process the device set in the low resistance state and it is possible to cycle the memory cell from the low resistance state.

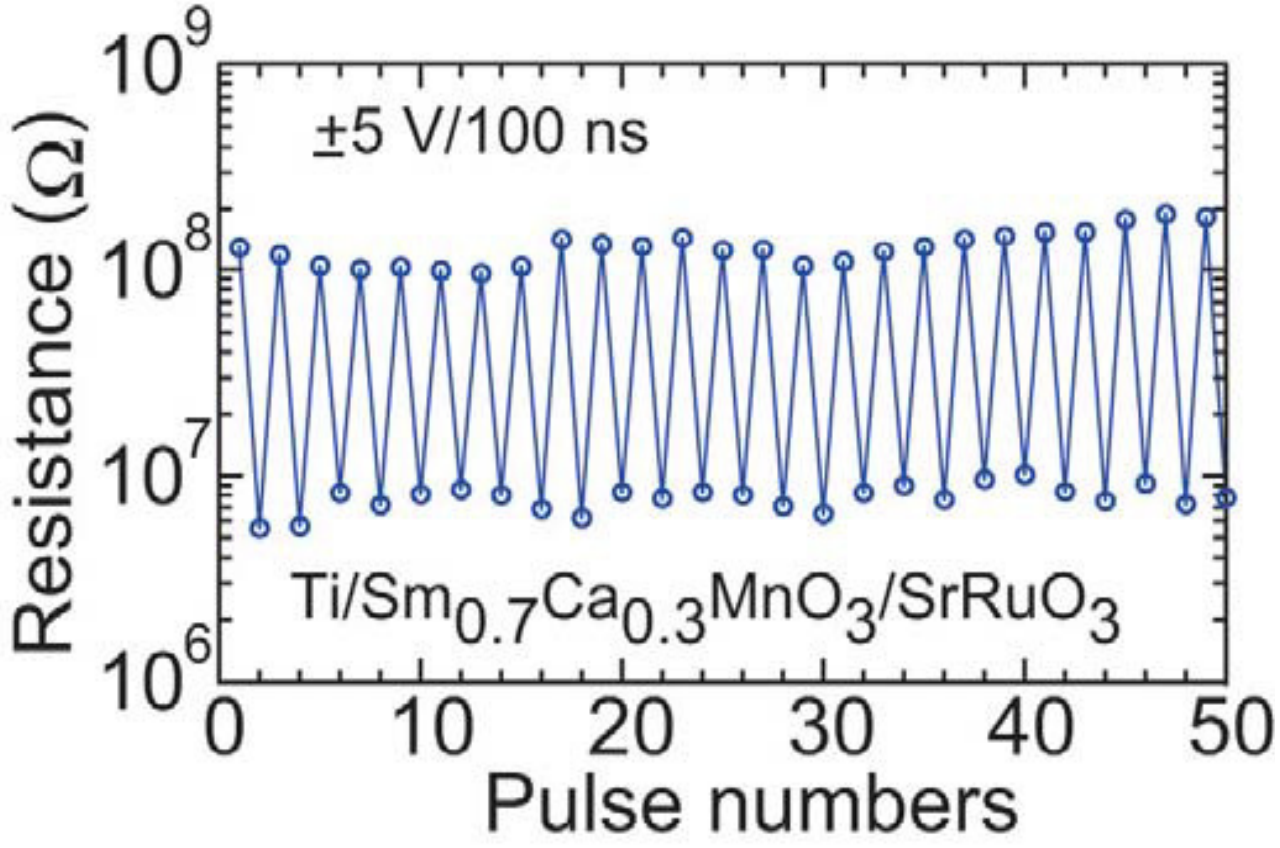

Figure 2. Resistive switching in Metal/Oxide/Metal hetero structures by applying pulse voltage

Nanowires structuring has in recent time been employed as an interestingly new or unusual solution to exploit and enhance materials properties,ferroelectricity,piezoelectricity,electro-optics,non-linear optics and optical switching properties.

At the nanoscale level, resistive switching (RS) in oxides shows peculiar features, it shows reversibility and non-volatile properties in metal-oxides-metal (MOM) structures ,basically between high resistance and low resistance state (HRS and LRS) respectively which are prompt by electric pulses. Segment of MOM nanowires present significant advance all –oxides nanowire in the following ways;

1. The integrated metal electrodes allow the tuning of the oxide thickness independently from the total nanowire length.

2. There is a precise definition of the geometry of the cell and of the internal electric field distribution.

Hence, resistive switching random access memories (ReRAMs) have been considered as emerging technologies by International Technology Roadmap for semi conductors due to their potential for downscaling and low power operation.

Due to the resistive change of the insulator in a metal–insulator-metal (MIM) structure, resistance random access memory (ReRAM) possesses the advantages of low power consumption, high operation speed, non destructive readout, simple structure and good scalability, which is highly competitive candidate for the generation of nonvolatile memories.

While DRAM is a volatile technology and due to its charge- base switching mechanism its scalability is limited, while on the other hand ,flash is the dominant non- volatile memory

technology with a good scalability down to 22nm node. The major drawback of using flash memory read/write operation s is that they are basically slow and the flash memory has a finite number of program-erase cycles (referred as P/E cycles). Most commercially available flash products are guaranteed to withstand around 100,000P/E cycles, before the wear begins to deteriorate the integrity of the storage.

Therefore a lot of new memory concept are investigated that combine non-volatile data storage with high durability and scalability than the traditional flash memory concept. Scalability is in particular one of the most important requirement for the new standard of memories; while embedded memory applications required a good compatibility with standard semi conductor process (C- Mos technology).Read/write operational speed must be in the range of ions for 1byte with lower power consumption, especially important for mobile application. The innovation technology of non-volatile memory technology of non-volatile memory technologies appeared about 20years ago with the following concept;

- Magnetic Resistive RAM : Non-volatile memories that has been under development since the 1990s.Unlike conventional RAM chip technologies in MRAM data is the not stored as electric charge or current flows,but by magnetic storage elements.The elements are formed from two Ferromagnetic plates,each of which can hold a magnetic field,separated by a thin insulating layer.

- Ferroelectric Random Access Memory(FeRAM): This is a non-volatile memory with similar structure of traditional Dynamic RAM (DRAM) with the presence of ferroelectric layer which gives the non-volatile property to the device.

- Phase – Change RAM (PRAM) :This is a kind of non-volatile memories which exploit the unique behaviour of Chalcogenide glass.Heat produced by the passage of an electric current switches this material between two states,crystalline and amorphous which exhibit different electrical optical and thermal properties.

There have been a lot of studies in ReRAM application including the perovskite oxides such as $SrZrO_2$, Pt-xcxxMnO_3, doped and undoped transition metals oxide (TMOs). Because of their structure, easy fabrication process and excellent compatibility with current complementary metal oxide semiconductor (CMOS) technology. Many TMOs have been reported to exhibit resistive switching phenomena such as NiO, ZnO, Cu_2O, ZrO_2 TiO_2, and Nb_2O_5.

It is thought that resistive switching is an intrinsic property of TMOs, and all doped and undoped TMOs can exhibit resistive switching (RS), which is the reversible in metal-oxide-metal (MOM) structures between high resistance and low resistance state (HRS and LRS respectively) driven by electrical pulses. More so, segmented MOM nanowires present significant advances over all-oxide nanowires, the integrated metal electrodes allow the tuning of the oxide thickness independently from the total nanowire length, as well as a precise definition of the geometry of the the cell and of the internal electrical field distribution and for these reasons, they give the way toward the investigation of basic (RS) mechanisms at the nanoscale level.

Resistive random access memory (RRAM) or (ReRAM) is a new non-volatile memory type first developed by a number of companies. The technology bears some similarities with Conductive-bridging Ram(CBRAM) and Phase change memory. Different forms of ReRAM have been disclosed base on different dielectric materials, spanning from the perovskite to transition metals oxides to Chalcogenides.

The basic idea is that a dielectric, which is normally insulating can be made to conduct through a filament or conducting path formed after application of sufficiently high voltage .This conduction path formation can arise from different mechanisms, including defects metal migration etc. Once the filament is formed, it may be reset (broken, resulting in high resistance) or set (re-formed, resulting in high resistance)by an appropriately applied voltage. The switching mechanisms itself can be classified in different dimension. First there are effects where the polarity between switching from the low to the high resistance level (reset operation is reversed compare to the switching effects where both set and reset operations require the same polarity but different magnitude.

Another way to distinguish switching effects is base on the localization of the low resistance path. Many resistive switching effects shows a filamentary behaviour where only one or few very narrow low resistive paths exist in low resistive state.

Material Systems for Resistive Memory Cells;

1. Phase change chalcogenides like $Ge_2Sb_2Te_2$ or AgInSbTe.
2. Binary Transition metal oxide like NiO or TiO_2
3. Perovskites like $Sr(Zr)TiO_2$ or Pcmo
4. Solid –State electrolytes like GS, GSe or Cu_2S
5. Organic Charge transfer complexes like CuTCNO.
6. Organic donor-acceptor system like AlAlDCN.
7. Various molecular systems.

Finally my major concentration in will revolve around this novelty Binary Transition metal oxides; NiO, ZnO, Sn_2O, Cu_2O, and TiO_2.

2.0 State of the Art on Electrochemical Synthesis of Resistive switching Materials for ReRAM

2.1. Synthesis of Nickel Oxide Nanowire through Electrodeposition Route

Appling a unique combination of template-based synthesis method involving anodization, electroplating and selective oxidation, the synthesized engineered metal-oxide –metal (MOM) hetero-junction Au-NiO-Au system for possible use in resistive switching application. The template-base synthesis method applied is really generic and has the potential to provide control over the structure and characteristic of the resulting MOM nanowires.

Here, Au-NiO-Au systems are synthesized using a unique combination of previously developed template-based. Initially, the all-metal Au-Ni-Au nanowires were electrodeposited inside the nano holes of anode aluminum oxide (AAO) template. In the present study, a novel procedure to synthesize ordered arrays of MOM nanowires with measurable switching properties potentially down to the single nanowire is described. MOM nanowires arrays were fabricated by electrodeposition of Au/Ni/Au multilayers into AAO templates (hexagonally ordered pores having diameter of around 50 nm and interpore distance of around 100 nm), followed by mechanical polishing and chemical etching of the AAO template and in-situ thermal oxidation. The thickness of both the NiO layer and the Au electrodes was controlled down to the nanometer level. The resistive switching behavior of Au(15µm)/NiO(100 nm)/Au(15µm) arrays was assessed by means of C-AFM. This procedure can be considered in full details by following step by step processes involved.

2.1.1. Fabrication of AAO Template For NiO Synthesis.

The AAO templates were prepared using the Masuada method. There, high- purity Al foils of 100µm thick were anodized in the 0.3m Oxalic acid under 40v direct current (dc) at $18^{o}_{C.}$The Membranes were treated with a saturated solution of $HgCl_2$ to remove any Al metal. The membranes were then etched with $5wt^{o}/_{o}$ H_3PO_4 for 45mins to remove the barrier layer. Then the average diameter of the nanowire holes in the resulting AAO templates was 60nm.

More so, the manufacture of nanoporous anodic aluminium oxide (AAO) with ordered hexagonal arrays of uniform parallel nano pores has traditionally been made in one of three ways:

1. Mild Anodizing
2. Hard anodizing
3. Lithographically method

Mild anodizing produces self-ordered pore structures, but it is slow and only works for a narrow range of processing conditions .Hard anodizing, which is widely used in the aluminum industry, is faster, but it produces films with disordered and bigger pore structures. Lithographically method, which is an imprint step to produce a periodic array of indentations in either the Al2O3 layer or in a polymeric layer or photo resist layer.

A novel approach termed "pulse anodizing" that combines the advantages of the mild and hard anodizing processes. By designing the pulse sequences it is possible to control both the

composition and pore structure of the anodic aluminum oxide as show in the diagram below.

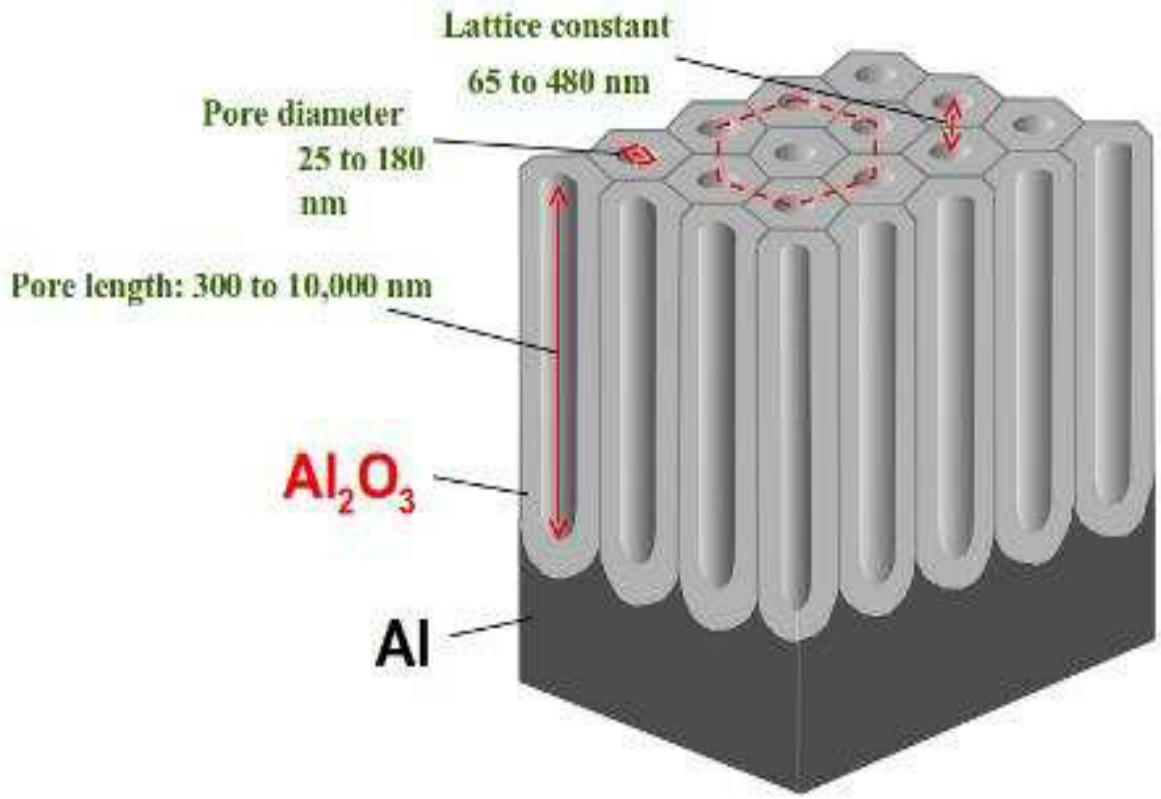

Figure 3:AAO Template showing the pore length,pore diameter and the lattice constant.

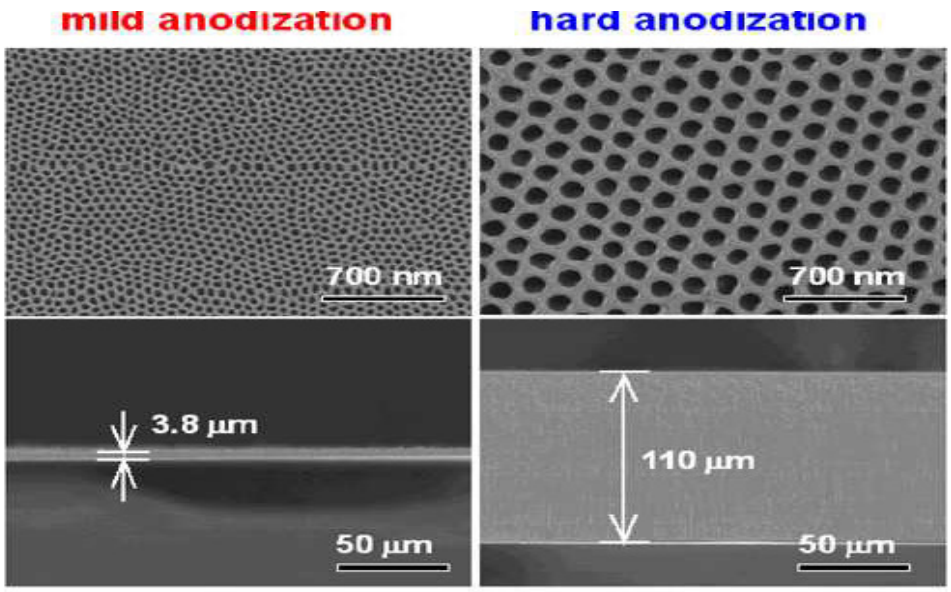

Figure 4: AAO Template showing the mild and hard anodization.

2.1.2. Practical Steps in Fabricating well ordered AAO Template

1. Cleaning the substrate surface. This could include using a simple solvent or, for some types of substrates, an electro polishing

2. Oxidizing the aluminum at a constant voltage in an oxalic acid C2H2O4 (0.3M in our lab) solution at low temperature (around 1°c) for approximately 21 hrs (our lab 3hours)

3. Removing the initial anodic oxide layer, by dipping in an acid mixture (1.8%chromic acid (H2CrO 4) and 6 wt% phosphoric acid, H3PO4) at an elevated temperature, around 65°for 20 hours. This yields a textured pattern of concave depression on the aluminium surface.

4. Completing a second anodizing of the textured aluminum by using the same experimental conditions as the first anodizing .This process results in the ordered holes (see in Figure 1) fabricated from each concave depression.

5. Removing the bottom part of the anodic porous alumina membrane by etching it in solution (HCl 20%, $CuCl_2$ (0.1M) for a short period of time to form a through-hole membrane.

6. The barrier layer was then removed in 6 wt % H_3PO_4 solution at 30°C. At this stage the pores are widened from 50 to 70 nm the time of opening is so important, giving more time make wider pores while giving less time make not enough opening. of pores

2.1.3. Electrodeposition Process of Nickel.

Prior to electroplating, one side of the AAO template was sealed by thermally evaporating a 0.5-µm Au thin film. Then, the Au nanowire segment was the electroplated using Orotemp 24 solution (Technic Inc) with a pit foil as the anode. The Ni segment was electroplated using 0.5M

nickel II sulfate (Alfa Aesar) with a nickel foil as anode. Finally, the Au nanowire segment was electroplated using the same condition as before.

Another way of electrodeposition into AAO templates (Nanomaterials Srl) having hexagonally ordered pores with average diameter of around 50 nm, interpore distance of around 100 nm, and average porosity of around 22% and before the electrodeposition of the Nickel nanowires, the bottom surface of the AAO templates was coated by sputtering with a 100 nm thick Au film.

Then, a nickel sulphate-based electrolyte (Watts bath) containing 300 g/l $NiSO_4$ • 6H2O, 20 g/l $NiCl_2$ • 6H2O, 40 g/l H3BO3 was used to carry out the electrodeposition of the Ni layers.The pH of the electrolytes was 3.7. The electrodeposition was carried out at 45 °C in galvanostatic mode at12 mA/cm_2.

2.1.4. The Oxidation Process of Elecrodeposited Ni to NiO

After the electrodeposition of the Au/Ni/Au nanowires, the AAO templates were mechanically polished and chemically etched to reduce the thickness of the AAO membrane and expose the nanowires from the AAO surface. Mechanical polishing was done by lapping the samples at 250 rpm using diamond powder paste with particle size about 1µm and hardness of 8400 HV. Mechanical polishing was carried out by hand applying a gentle pressure on the samples. Chemical etching was carried out in phosphoric acid: chromium trioxide=6%:1.8% solution at 40 °C for different etching times. Au/Ni/Au nanowires arrays embedded into AAO templates were finally subjected to a thermal oxidation process at 400°C in controlled oxygen atmosphere in order to convert the Ni layers into NiO.

Another possibility is when the release all metal nanowire of Au-Ni- Au were placed on high purity pt foils and subjected to heat treatment in air .The Au-Ni-Au nanowires undergo only a

one-step heat treatment of 600^{o}_{C} for 2hours in which the Ni was oxidized to NiO, since the melting point of Ni is (1455^{o}_{C}) while it's alloys (955^{o}_{C}). So with Au are much higher than the oxidation temperature. The entire synthesis process is shown in figure 5

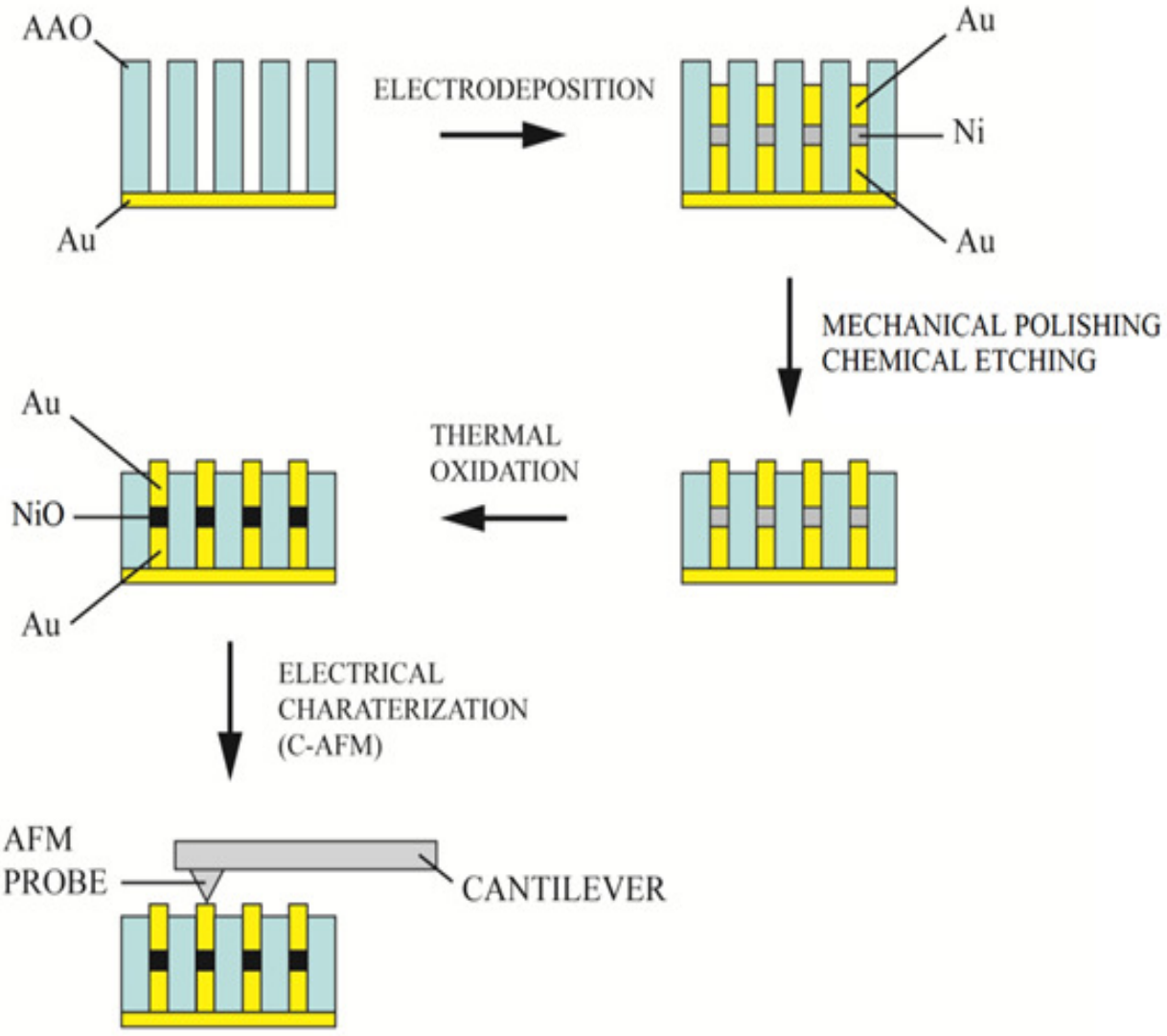

Figure 5: Entire Synthesis process of NiO nanowires .

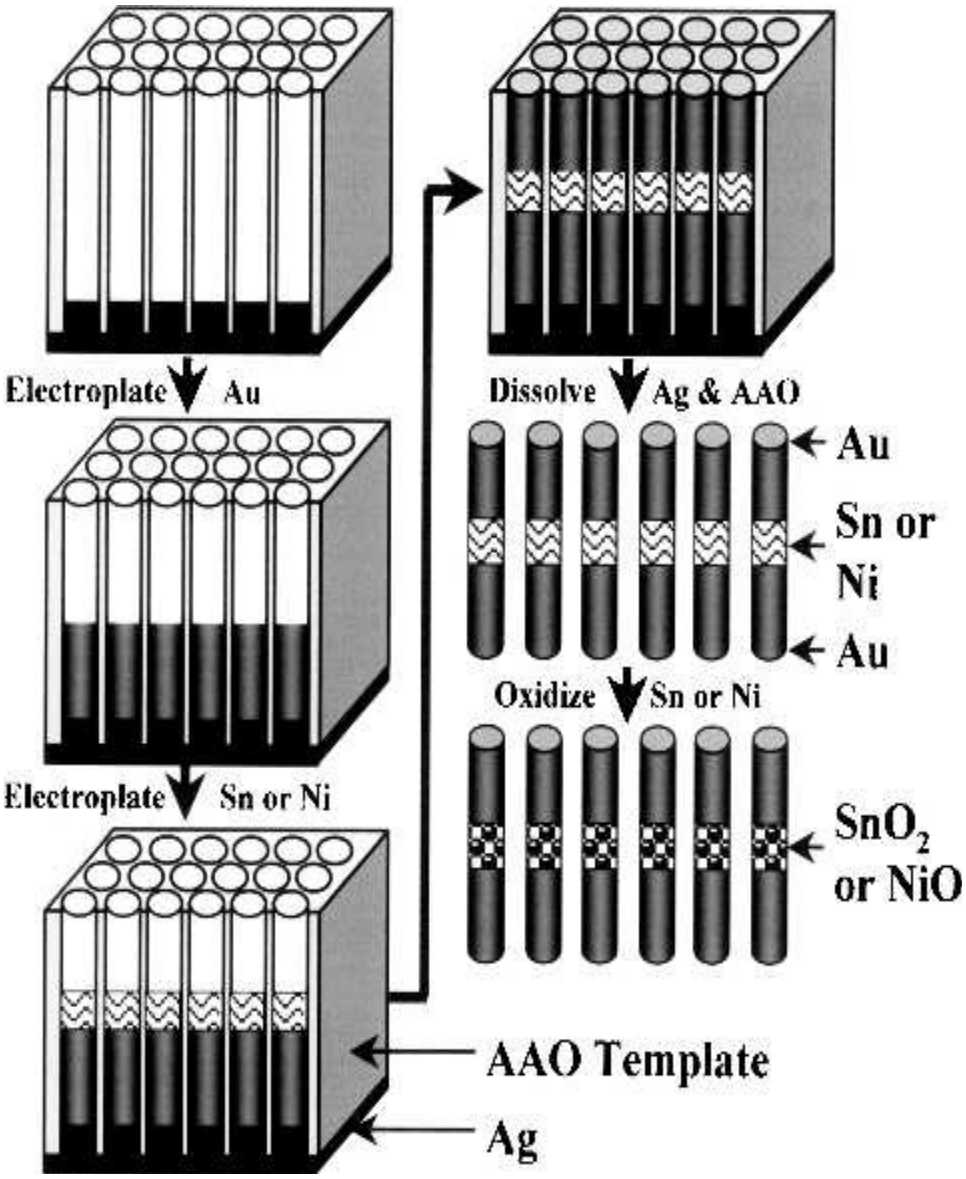

Figure 6: Schematic illustration of the multi-step synthesis process used to synthesize Au–NiO–Au nanowires.

2.1.5 Characterisation of the Au-NiO-Au

The first stage of the process is to determine the thickness of the AAO templates by means of Fischer DualScope® FMP100 with FTA 33 sensor. The morphology and surface topography of

the nanowire arrays which were investigated by means of Scanning Electron Microscopy (SEM–Zeiss® EVO 50) equipped with field emission source, operated at 20 kV accelerating voltage. The Atomic Force Microscopy (AFM – NTMDT® Solver ProM) and Transmission Electron Microscopy (TEM) using a Tecnai High Resolution-TEM equipped with a field emission gun and spherical aberration corrector, operating at 200 keV were also used.

The second stage of the process is to carry out the TEM characterizations, and to do that, the thermally treated nanowires were released from the AAO templates. The dissolution procedure involved the etching of the sputtered Au layer with Aqua Regia, followed by immersion in 1 M NaOH for 10-15 min (Ni nanowires) or in phosphoric acid:chromium trioxide=6 wt%:1,8 wt% solution at 60 °C for 60 minutes . The nanowires were then collected, rinsed several times with distilled water and ethanol 99%, and finally stored in ethanol. To accomplish the TEM characterization, a drop of the nanowires-ethanol suspension was spread onto standard TEM Carbon-Copper grids and left to dry before observation.

On the other hand, figure 6 shows TEM bright-field images of an isolated Au–NiO–Au nanowire synthesized inside an Anopore AAO template, at low and high magnifications. The selected-area electron diffraction patterns (SAEDP) in Figure 7 confirms the oxide part of the nanowire (light) to be polycrystalline cubic NiO (referred to as bunsenite) as shown below.

The phase structure and texture of the nanowires were determined both by X-ray diffraction (XRD) with Cu K radiation at 1.54 Å and a powder goniometer (Philips PW- 1830), and by selected-area electron diffraction patterns (SAEDPs) of TEM bright field images.

Another aspect is electrical characterization of the nanowire arrays that was obtained by means of C-AFM measurements performed by using a Veeco Dimension 3100 with a Nanoscope V

controller in air at room temperature with commercial doped Pt/Ir coated tips. All tips were by Nanosensors . And the Measurements were carried out at room temperature

EDS also confirmed the presence of Ni and O in the light (NiO) segment, and Au in the dark (Au) segments. The overall length of the MOM nanowire is over 7μm, and the diameter of the Au part of the nanowire is ~270 nm. The NiO segment of the MOM nanowires is ~300 nm in diameter and ~200 nm long.

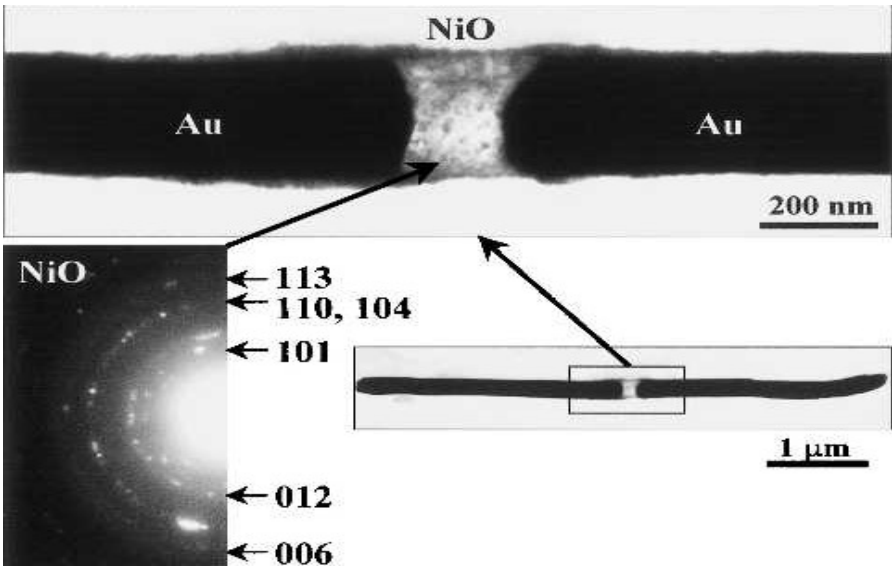

Fig 7: TEM bright-field micrographs showing an isolated Au–NiO–Au nanowire synthesized inside an Anopore AAO template, at low (bottom right) and high (top) magnifications. The dark regions are Au and the light region is NiO, the latter identified using corresponding SAEDP (bottom left).

2.2. Synthesis of Tin Oxide (Sn_2O) Nanowire through Electrodeposition Technique

The synthesis of engineered metal-oxide-metal (MOM) heterojunction nanowires in the Au-SnO_2-Au system for possible use in resistive random access memory. Base on the fact that

nanoscale segment of a functional oxide is sand switched axially between two similar or dissimilar noble-metal nanowires.

Here Au-SnO_2-Au system is synthesized using a unique combination of previously developed template-based. All-metal Au-Sn-Au nanowire were electroplated inside the nanoholes of anodic aluminum oxide (AAO) templates, as shown schematically in Figure 4 above. The nanowires were then released by dissolving the AAO templates and the dispersed nanowires were heat-treated to selectively oxidized the Sn segment to SnO_2.

2.2.1. Preparation of AAO Template for the Synthesis

The AAO templates were prepared using the Masuda method. There, high- purity Al foils of 100µm thick (Alfa Aesan,Wand hil,MA) were anodized in the 0.3m Oxalic acid under 40v direct current (dc) at 18^{o}_{C}.The Membranes were treated with a saturated solution of HgCl2 to remove any Al metal. The membranes were then etched with $5wt^{o}/_{o}$ H3PO4 for 45mins to remove the barrier layer. Then the average diameter of the nanowireholes in the resulting AAO templates was 60nm.

2.2.2. Electrodeposition Process

One side of the AAO templates was pre-formed using the method pioneered by Moskovite and coworkers and Martin and coworkers. With the Ag thin film serving as the cathode and Ag foil as the anode, a small segment of Ag (~0.5µm) was electroplated using the 1025 Ag solution. Then, the Au nanowire segment was then electroplated using the Orotemp 24 solution with a pt foil as the anode. The Sn segment was electroplated using 3M solution of tin (II) chloride with Sn foil as the anode. Finally, the Au nanowire segment was electroplated using the initial condition. Then, the AAO template was dissolved in 3M NaoH, while the solution was being dilute and ultrasonicated.

2.2.3. Oxidation Process of the Deposite

The released all-metal nanowires were place in high purity pt foils and subjected to heat treatment in air. The Au-Sn-Au nanowires were subjected to a two-step heat treatment.

1. To 197^{o}_{C} for 0.5hours which is low temperature heat treatment ,below the melting points Sn (232^{o}_{C}) and its lowest melting alloy (217^{o}_{C}) with Au ,this is basically applied for converting the Sn to SnO.

2. To 650^{o}_{C} for o.5hours.This high-temperature heat treatment is for converting the SnO to $SnO_{2.}$

2.2.4. Characterisation of the Au-SnO_2-Au

The resulting Au-SnO_2-Au MOM nanowires were dispersed in de-ionized water or ethanol .Then drops of solution containing the MOM nanowires were placed on 3-mm transmission electron microscope (TEM) grid and dried. The nanowires were then observed in either a JEM 2010 TEM (JEOL) or a CM-200 TEM (Philip; Eindhovin,the Netherlands) operated at 200kv.Both TEMs are equipped with atmospheric thin-window energy dispersive spectroscopy (EDS) system (phoenix EDAX Mahwah,NJ).Then considering the image of an isolated Au-SnO_2-Au nanowire synthesized inside an in-house prepared AAO template as show below.

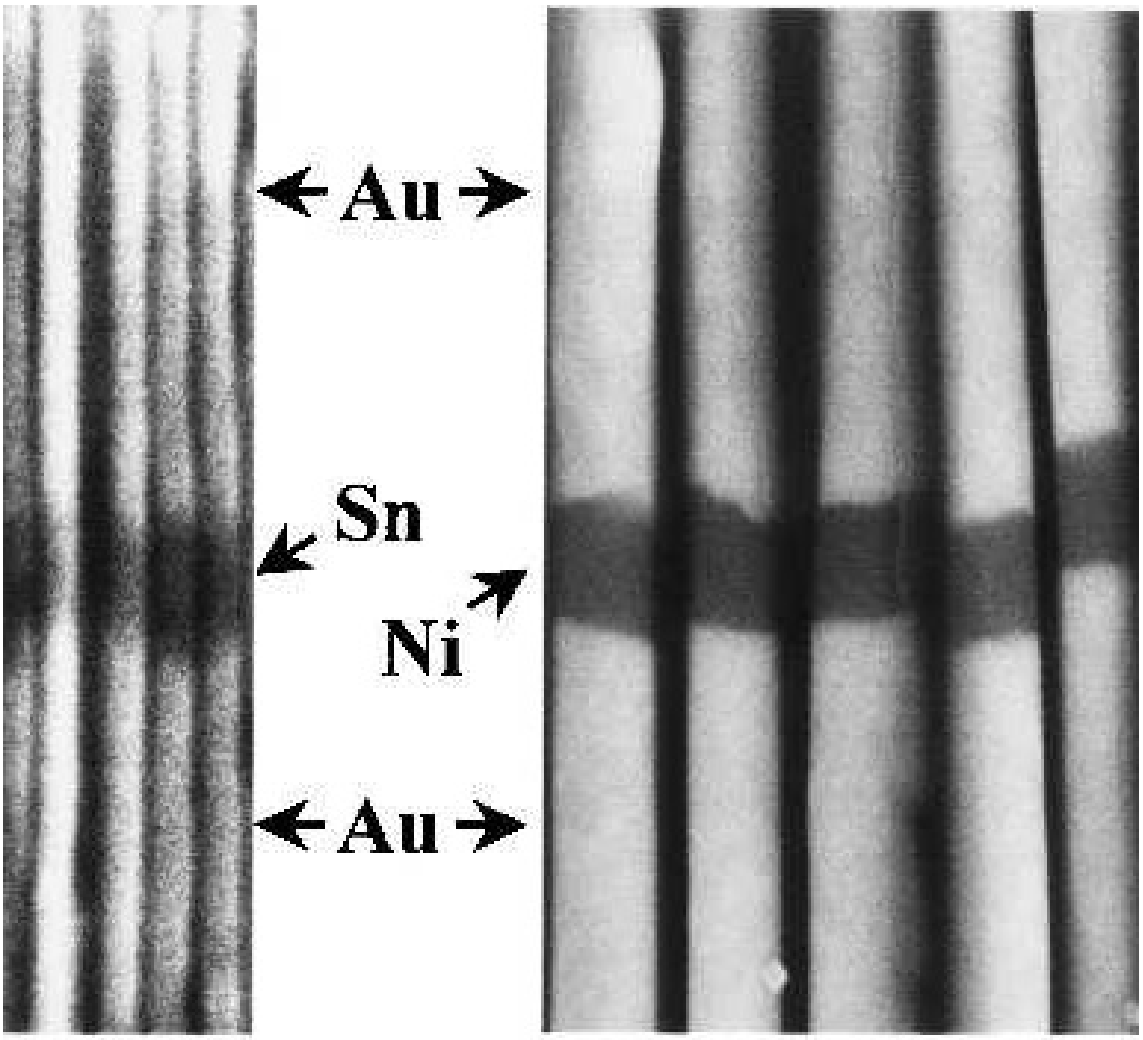

Figure 8: SEM Micrograph of all-metal nanowire of Au-Sn-Au inside fractured in- house-prepared AAO template.

More so ,the diagram below shows selected-area electron diffraction patterns (SAEDPs), which confirm the metal part of the nanowire (dark) to be Au, and the oxide part of the nanowire (light) to be polycrystalline tetragonal SnO2 (referred to as cassiterite or rutile). EDS also confirmed the presence of Sn and O in the light (SnO2) segment, and Au in the dark (Au) segments. The overall length of the MOM nanowire is over 2μm, and the diameter of the Au part of the nanowire is ~60 nm. The SnO2 segment of the MOM nanowires is ~60 nm in diameter and ~70

nm long. The highly jagged interface between Au and SnO2 observed in Fig.9 appears to be due to the diffusion of Au in Sn prior to the oxidation of Sn, which has been observed by others in Au–Sn–Au nanowires. At the first step of the oxidation heat-treatment (197 °C) the diffusivity of Au in Sn is estimated at 1.9 × 10−12 m^2 s^{-1},while the diffusivity of Sn in Au at the same temperature is almost 10 orders of magnitude lower at 6.2 ×10−22 m2 s−1.20 .

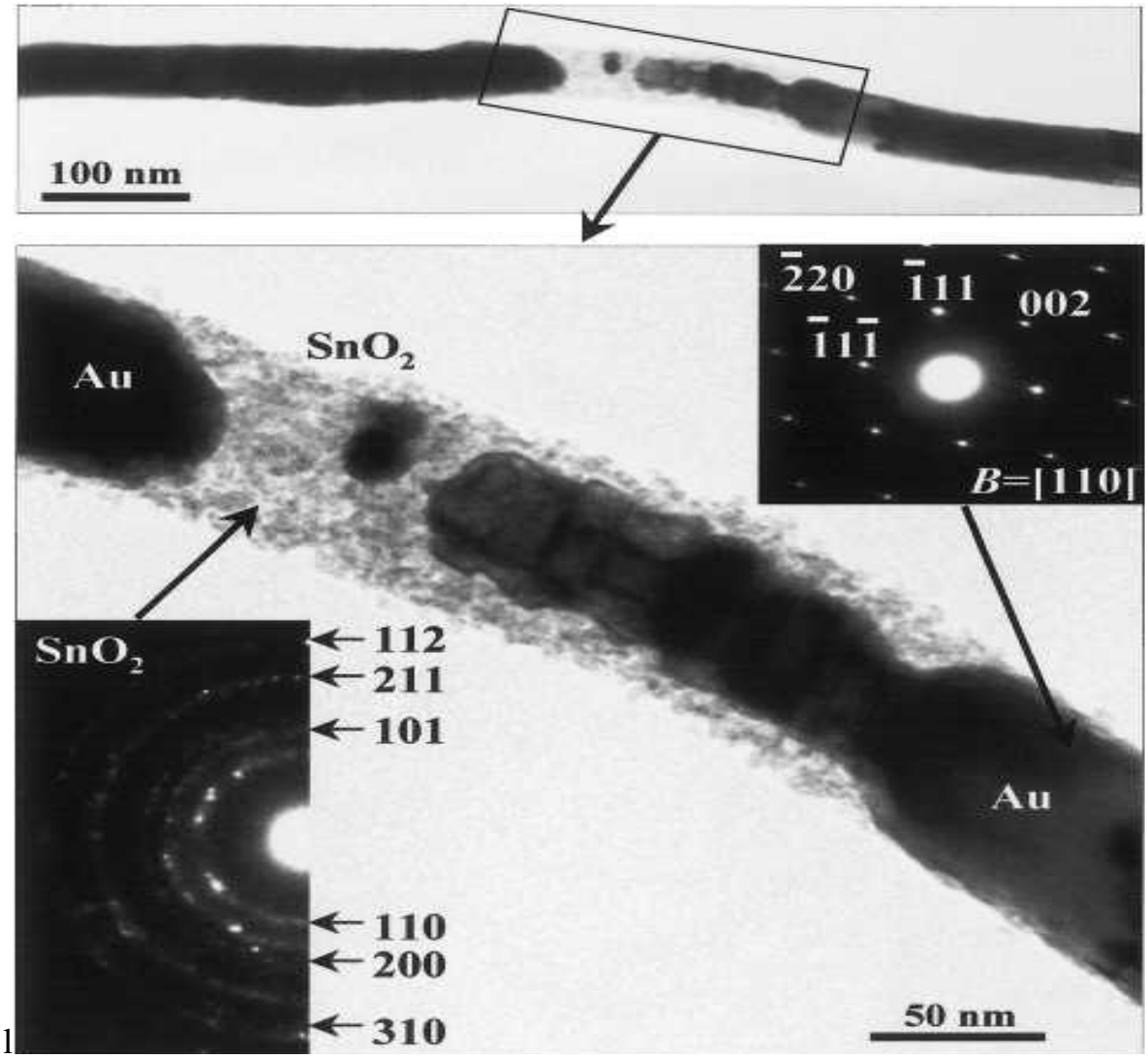

Fig 9: TEM bright-field micrographs showing an isolated Au–SnO2–Au nanowire synthesized inside an in-house prepared AAO template.

The diagram below also shows a high resolution TEM image of a polycrystalline SnO_2 segment, revealing the grains ranging from 5 to 10nm .

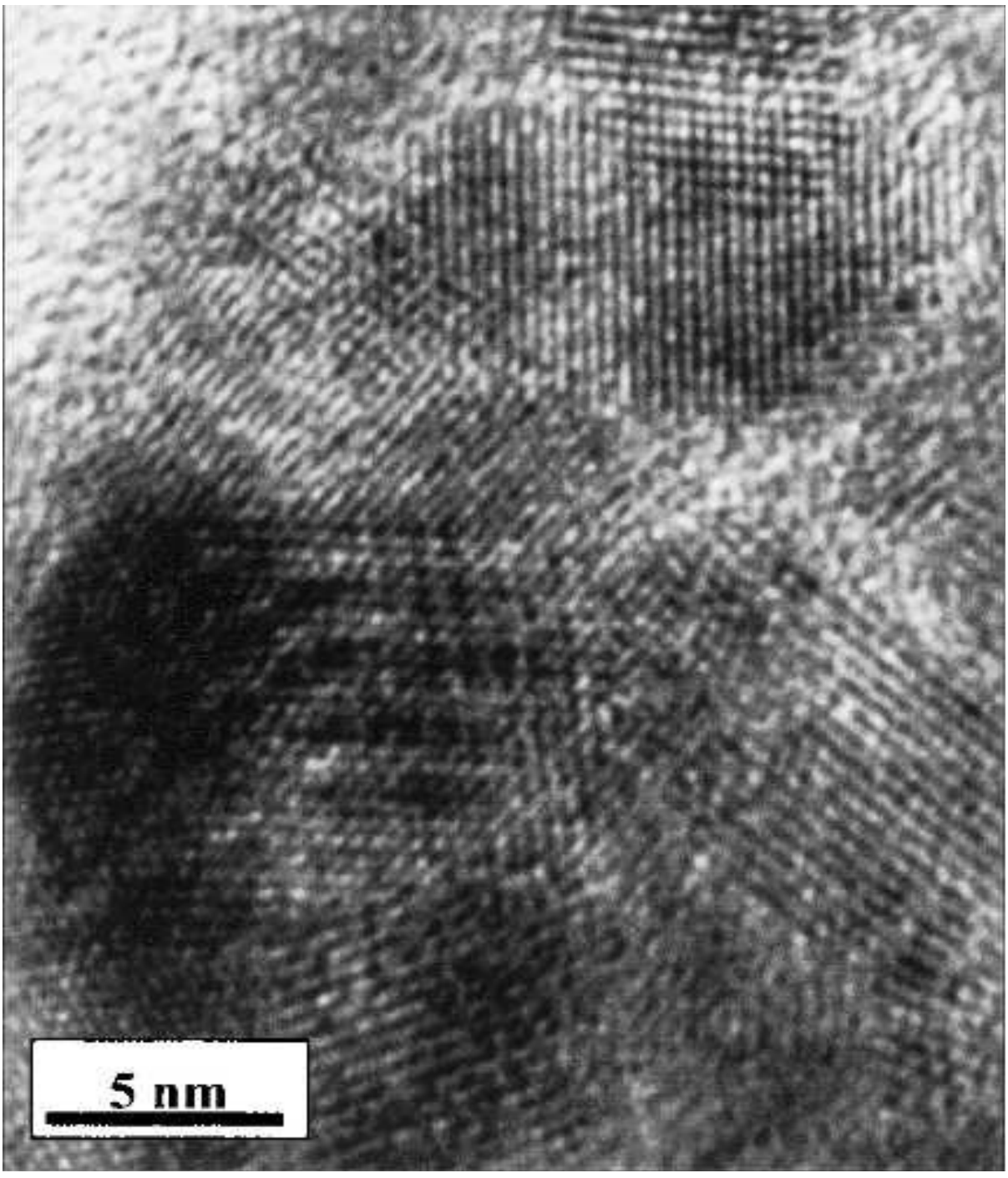

Figure 10: High-resolution TEM micrograph of the SnO2 region in the Au–SnO2–Au nanowire

The diagram clearly shows the SEM micrographs of an isolated Au–SnO2–Au nanowire synthesized inside an Anopore AAO template.

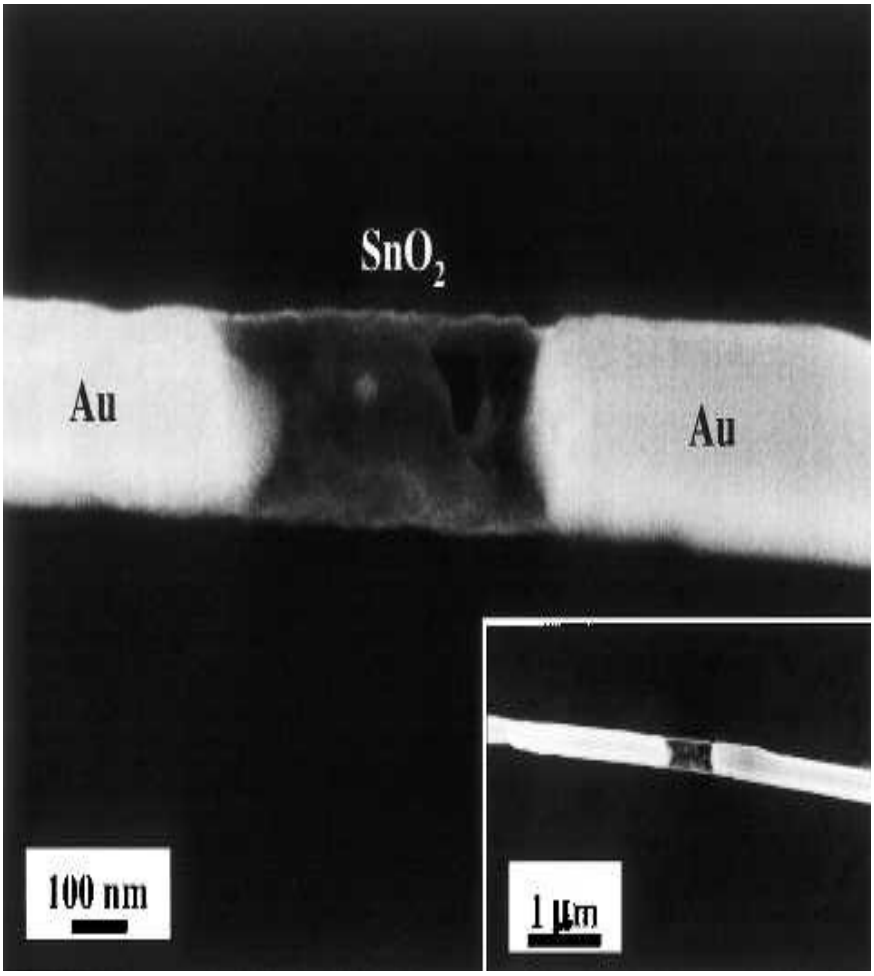

Figure11: micrographs showing an isolated Au–SnO2–Au nanowire synthesized inside an Anopore AAO template at high and low inset) magnifications.

The overall length of this MOM nanowire is over 10µm, and the diameter of the Au part of the nanowire is ~220 nm. The SnO2 segment of the MOM nanowires is ~220 nm in diameter and ~400 nm long.It is also observed that Au–SnO2 interface is not as jagged due to the longer diffusion lengths involved Like what is observed in the in figure.

2.3 Synthesis of Cu_2O Nanowires Via Electrodeposition Route for ReRAM Application.

This involves the fabrication of cuprous oxide (Cu_2O) nanowires using a home-made nanoporous alumina template by electrodeposition technique.

The Cuprous oxide nanowires were deposited galvanically into a hexagonal nanoarray alumina membrane using the three-electrode system;counter electrode and reference electrode were platinum mesh and saturated calomel electrode (SCE) respectively.

2.3.1. Electrodeposition Bath Composition

The preparation of electrodeposition bath took place by using 45g of 99.9995$^{o}/_{o}$ $CuSO_4$ (Aldrich) which was dissolved in 75ml of 88 $^{o}/_{o}$ lattic acid (Aldrich) and the copper ions stabilized by complexing with lactate ion. 5M NaOH (Aldrich) aqueous solution was added to adjust the PH to 9.A current density of -0.5mA/cm^2 and the bath temperature of 65^{o}C was constantly maintained during the experiment.

2.3.2. Electrodeposition Procedures

By analysis and reference to previous studies, we first tried to deposit Cu2O nanowires on Ni nanowires inside alumina templates and Fig. 12 shows Cu2O–Ni nano-junctions formed in the alumina template. First of all, Ni is filled into the alumina template and Cu2O is deposited onto the Ni nanowires in sequence. When a current density of −20 mA/cm2 was applied for 35 min, the length of the Ni nanowires is ca. 28 mm with a deposition rate of 0.8 mm/min. Considering the 200 nm diameter of Ni nanowires; its aspect ratio is 112. Then, Cu2O nanowires with about 4.0 mm length were successfully grown on Ni with a deposition rate of 0.017 mm/min, which is 42 times slower than the rate of Ni deposition.

However, we find it interesting that, to deposit the same aspect ratio of Ni and Cu2O nanowires, Cu2O consumes a cathodic charge of 7.2 C and it is ca. seven times less than that required for Ni preparation s 48 Cd. That is, the difference of the aspect ratio between Cu2O and Ni is in good agreement with the difference of charge consumed between Cu2O and Ni

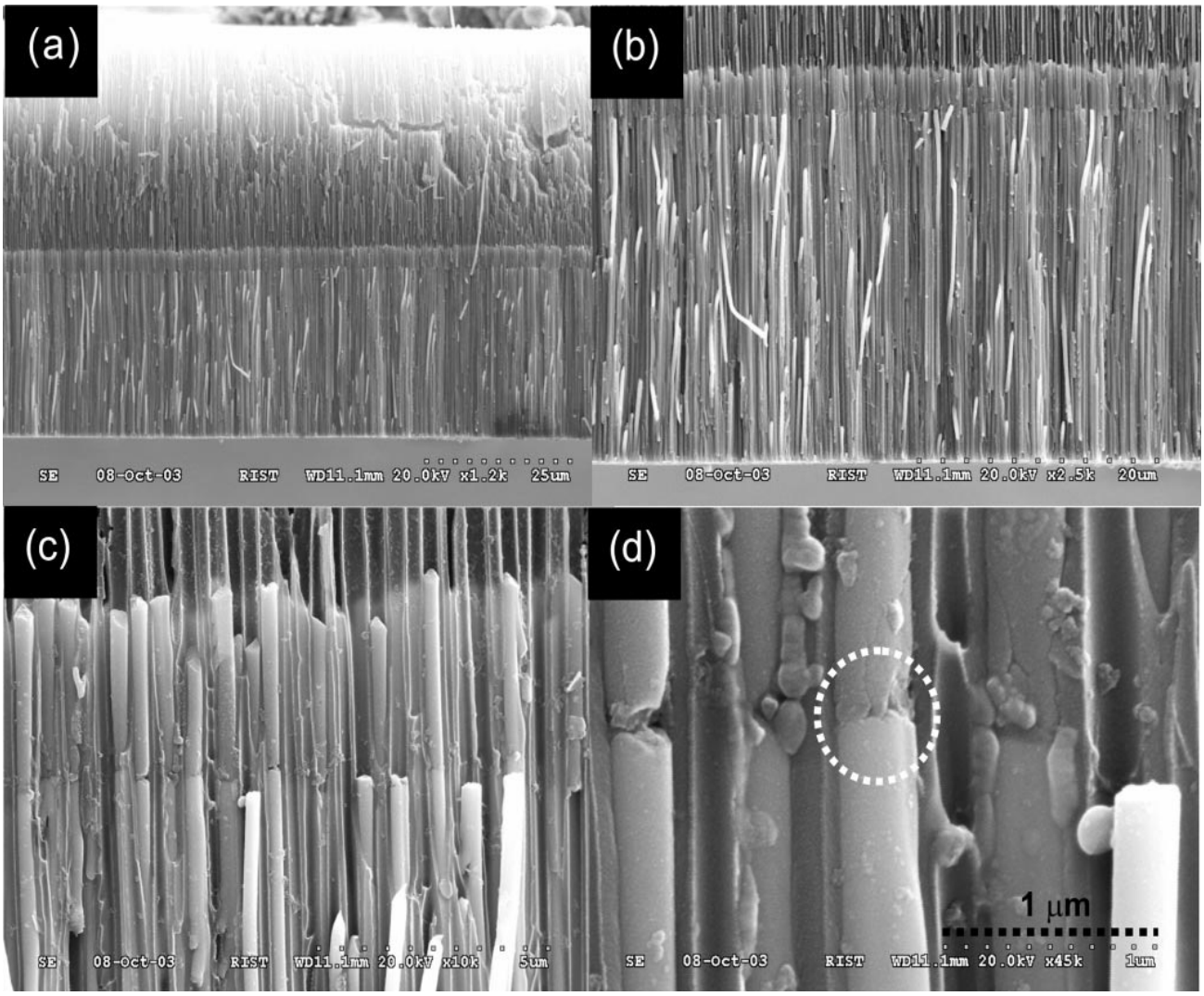

Figure 12: SEM observations of Cu2O nanowires on Ni nanowires in an alumina template with different magnifications. Cu2O preparation in $CuSO_4 \cdot 5H_2O$ + Lactic acid + 5 M NaOH at −0.5 mA/cm^2 for 4 h. Electrodeposition of Ni from $NiSNH_2SO_3d_2 \cdot 4H_2O$ + boric acid at −20 mA/cm^2 for 35 min.

2.3.3. Characterization of the Electrodeposited Material

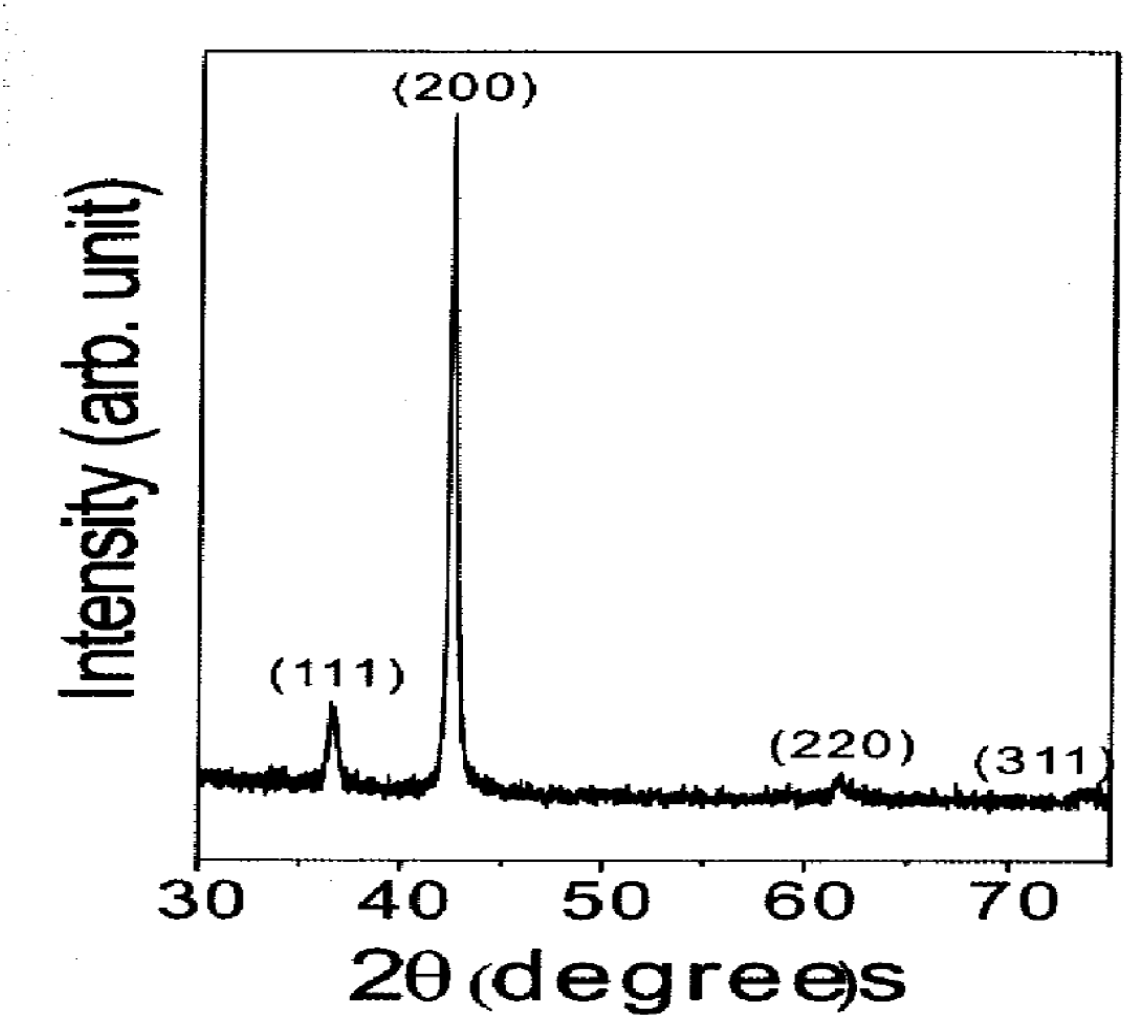

Figure 13: XRD pattern of a sample of Cu_2O nanowires in the alumina template prepared by the electrodeposition method at $65^{o}_{C.}$

2.4. Synthesis of Zinc Oxide Nanowire through Electrodeposition Route

2.4.1. Electrodeposition Process

The electrolyte for ZnO electrodeposition was 0.1 M zinc nitrate Aldrich dissolved in tridistilled water. A saturated calomel electrode SCE and platinum mesh were employed as reference electrode and counter electrode, respectively. A potentiostat-galvanostat (EG&G PAR 273A) was used to apply an optimal potential of −1.0 V and a current density of −0.5 mA/cm2 for the

deposition of ZnO . The solution temperature of 65°C was maintained constant during the processes. ZnO was not formed on Ni nanowires, because the distance between the bulk solution and the conducting cathode Ni hinders the movement of zinc ions, stabilized in aqueous solution, to the Ni substrate.

Therefore, ZnO could be deposited onto the alumina template,not inside alumina template, and the deposition mechanism of ZnO formation. Thus, we performed the experiments with a smaller distance between the Ni cathode and the zinc nitrate bulk solution by preparing longer Ni nanowires of 50 mm length.zinc ion in aqueous solutions most probably exists as the tetra coordinate aquo ion, and we assume that its mobility to the cathode is much smaller than nitrate ions. Then the zinc ion complex near the top of the alumina template reacts with hydroxides ion and form zinc hydroxide . Zinc hydroxide precipitated on the alumina template becomes ZnO by a dehydration reaction as shown by the chemical equations.

1. $NO^{-3} + H_2O + 2e- \rightarrow NO^{-2} + 2OH^-$
2. $Zn^{2+} + 2OH^- \rightarrow Zn(OH)^2$
3. $Zn(OH)^2 \rightarrow ZnO + H2O$

2.4.2. The Characterisation of the Material

The surface morphology of the prepared nanowires was analyzed by field-emission scanning electron microscopy FE-SEM, Hitachi, S-4300. The crystallinity and quantitative analysis of the metal oxides was carried out using X-ray diffraction XRD, Phillips DY616 and energy dispersive X-ray spectroscopy EDX coupled with the SEM equipment Under the same conditions.

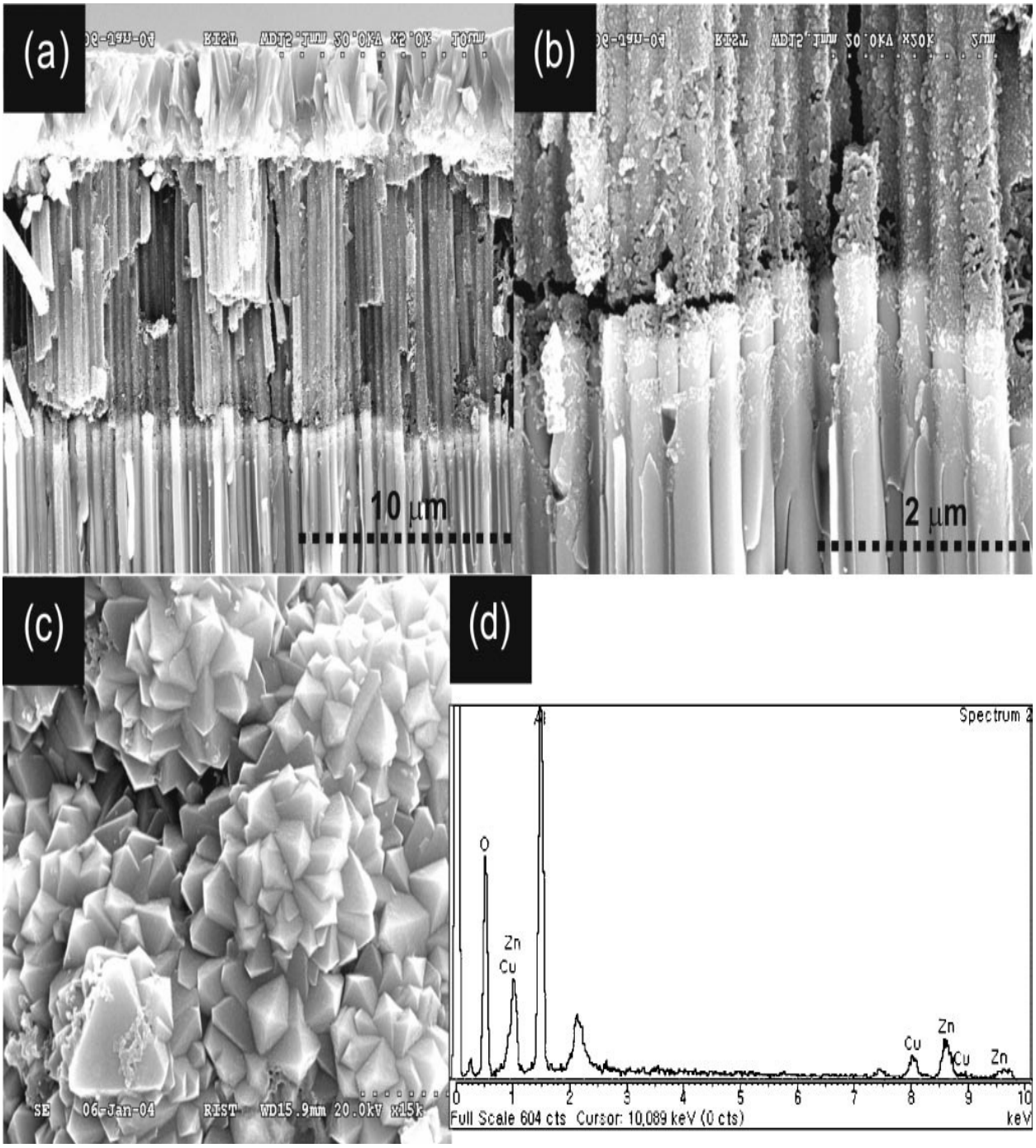

Figure 14: Morphological observations of nano-junction of Cu2O/ZnO on Ni nanowires with different magnifications. Cross-sectional views, top view, and EDX analysis of second region. Electrodeposition of Ni from NisNH2SO3d2·4H2O + boric acid at −20 mA/cm2 for 55 min. ZnO electrodeposition in 0.1 M ZnsNO3d2 with application of −1.0 V at 70°C for 60 min. Cu2O preparation in CuSO4·5H2O + Lactic acid + 5 M NaOH at −0.5 mA/cm2 for 4 h.

The diagram below also shows basically the morphological structure of ZnO and the EDX analysis of Zinc oxide nanowire on Nickel.

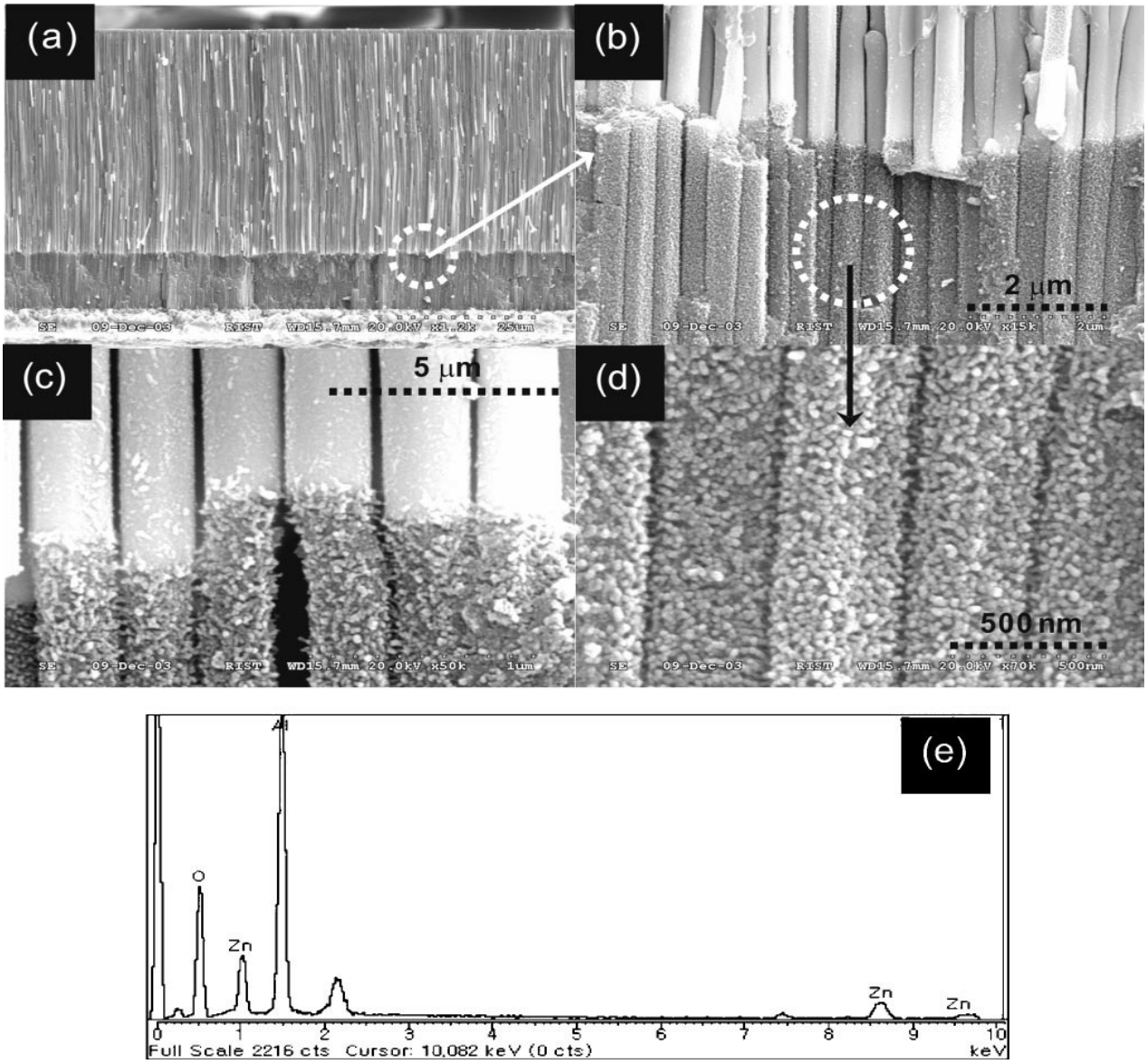

Figure 15 :(a-d) Morphological observations and EDX analysis of nanostructured ZnO on Ni nanowires with different magnifications. Electrodeposition of Ni from NisNH2SO3d2·4H2O + boric acid at −20 mA/cm2 for 60 min. ZnO electrodeposition in 0.1 M ZnsNO3d2 with application of −1.0 V at 70°C for 60 min.

2.5. Synthesis of Titanium oxide (TiO2) Nanowire through Electrodeposition

Due to the demands of TiO2 in different applications, simple and low cost techniques are required for thin film deposition. Chemical and electrochemical methods are emerging as important synthetic methods to thin films not only for their cost effectiveness but also for the high quality of the materials. These methods are suitable for large area and even for complex structures. In the present investigation, we report on the electrochemical synthesis of nanocrystalline TiO2 anatase thin films and powder. Characterizations were accomplished by using various techniques such as XRD, TEM, XPS, SEM, and AFM.

2.5.1. Electrochemical Bath Composition

The precursor bath consisted of 0.04 M TiOSO4,0.2MH2O2 and 0.1MKNO3 (pH ~ 2) solutions maintained at room temperature (25 °C) was used for electrochemical synthesis. The clear solution was used as electrolyte. A conventional three electrodes electrochemical cell was used for electrosynthesis. Saturated calomel electrode (SCE) was used as reference and all

the potentials were quoted with respect to this reference. The counter and working electrodes were platinium and Indium doped tin oxide (ITO) coated glass, respectively. The deposition was carried out by applying –1.2 V potential vs. SCE for 3 h. During deposition, the bath solution was continuously stirred. Typically 3 h deposition resulted in a smooth and flat film with a thickness of 50 nm. As a result of hydrolysis white amorphous titanium oxyhydroxide gel particles were observed in the bath after 3 h.

2.5.2. Heat Treatment of the Resulting Products

The formed gel powder in the bath was collected by filtering the solution. The films and the byproducts were annealed in air at 400, 450 and 500 °C temperatures. It was observed that annealing at 500 °C for 1 h had better cystallinity than others. Annealing treatment allowed converting the amorphous film into anatase-phase. The annealing temperature of 500 °C was chosen for further studies.

2.5.3. The Characterization of TiO2 formed

First, X-ray diffraction (XRD) spectra were recorded with an automated Bruker D8 advance X-ray diffractometer with the following characteristics: CuKa, k = 1.5406 Å, 40 kV, 40mA and 2h = 20–80°. Measurements for thin films were taken using a glancing angle detector at h = 1°. Steps and collection time were, respectively, 0.01° and 7 s. The average crystallite size was determined with the Scherrer's method associated with the Topas 1.0 software. The phase composition was identified using the program EVA (version 4.0) provided by Bruker diffractometer.

Secondly, Philips CM12 microscope operated at 120 kV was used for performing transmission electron microscopy (TEM). Axial illumination as well as the 'nanoprobe mode', with a beam spots size of 1.5 nm was used to identify diffraction of individual clusters. High resolution (HRTEM) images were digitally recorded by using a CCD camera.

Moreso, XPS measurements were performed using a Leybold EA11MCD spectrometer with an Mg Ka source at 1253.6 eV. The base pressure was 2 × 10−8 Pa. Peaks were fitted with Gauss–Lorentz shapes. Scanning electron microscopy (SEM) images were recorded using a LEO1530 (Gemini) FE-SEM microscope with Schottky field emission and acceleration voltage of 10 kV.

Then, Atomic force microscopy (AFM) images were recorded using the Nanoscope IIIa scanning probe microscope in a contact mode. The commercial n+-silicon cantilevers were used with a typical spring constant of 0.2 N/m in order to investigate the surface roughness.

TiO2 has three well-known phases namely: anatase, rutile, and brookite . Rutile and anatase are tetragonal whereas brookite is orthorhombic. Rutile is the only stable phase. Anatase and brookite are metastable at all temperatures, and can be converted to rutile after heat treatment at high temperature. Fig.17. shows XRD pattern of TiO2 films deposited on ITO substrates electrochemical method. ITO substrate was used as a reference.

Obviously XRD patterns do not shows any rutile or brookite peaks. Similar crystal structure was observed for electrodeposited films on ITO.We observed that low deposition rate was favored for the films on glass and quartz substrates hence the deposition was performed for 12 h in order to get thicker films for structural analysis. Furthermore, the collected by product from chemical bath showed polycrystalline nature with preferred orientation along (101) plane with anatase structure as shown in fig.18. Using Scherrer's formula, we evaluated the crystallites size along (101) orientation.

Crystallite size of 23 nm was estimated for electrodeposited films. Fig.17 and 18 show transmission electron micrographs of the TiO2 film deposited by electrochemical methods on ITO substrates. The images exhibited a spherical and elongated shaped particles with roughly uniform in size of about 20–30 nm. High-resolution TEM images shows clearly developed lattice feature (Figs. 17and 18) which indicates that each of these larger particles is an agglomeration of smaller particles, with nanostructured domain. Also, the Fourier transformation (Figures 17 and 18) leads to demonstrate the inter-planer distance (d-spacing) of 3.59 and 3.45 Å for

electrochemically deposited films. Comparing d-spacing with standard JCPDS data, we conclude that the anatase phase with specific orientation along (101) direction was observed.

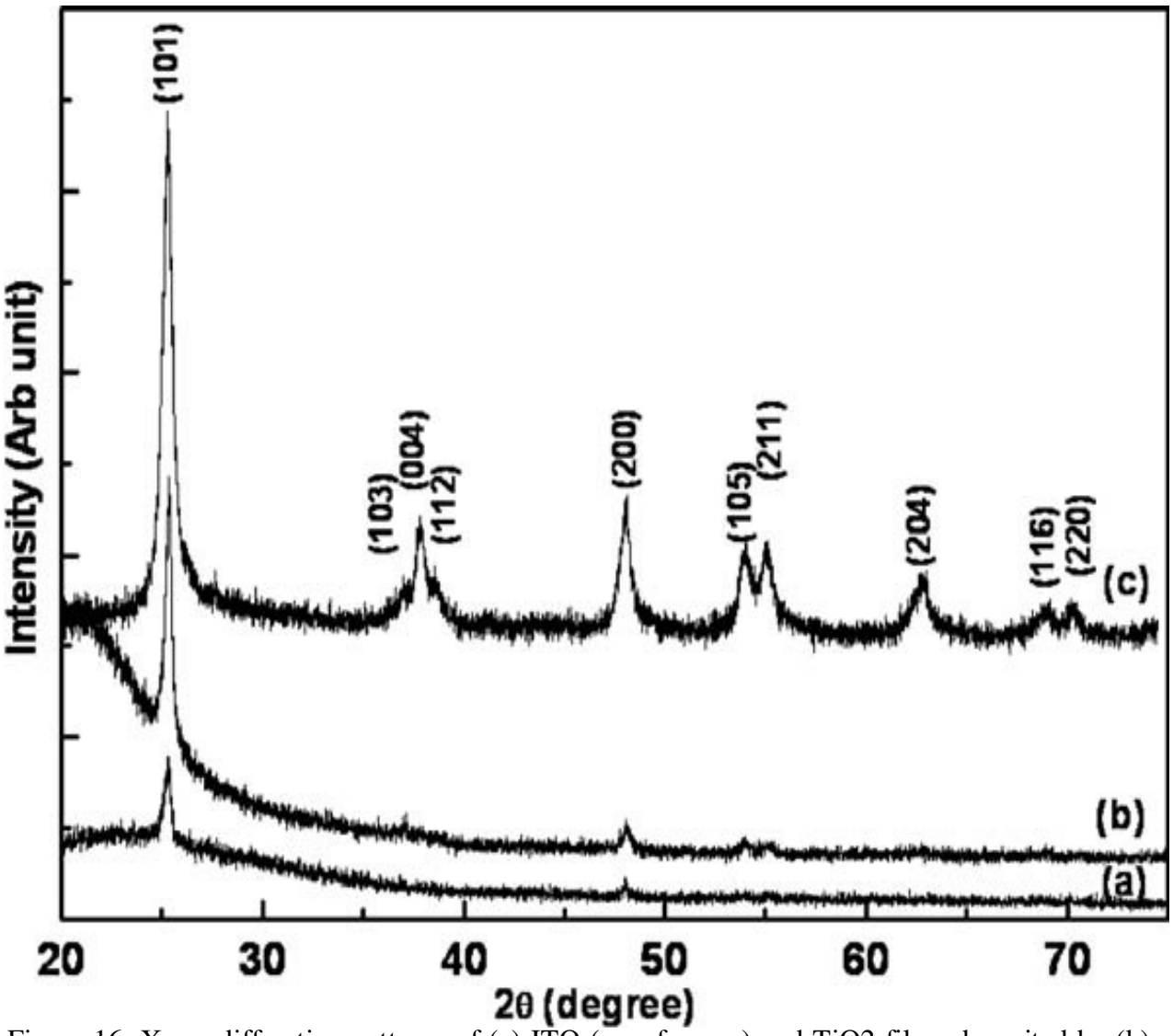

Figure 16: X-ray diffraction patterns of (a) ITO (as reference) and TiO2 films deposited by (b) chemical and (c) electrochemical methods on ITO substrate followed by annealing at 500 °C for 1 h in air

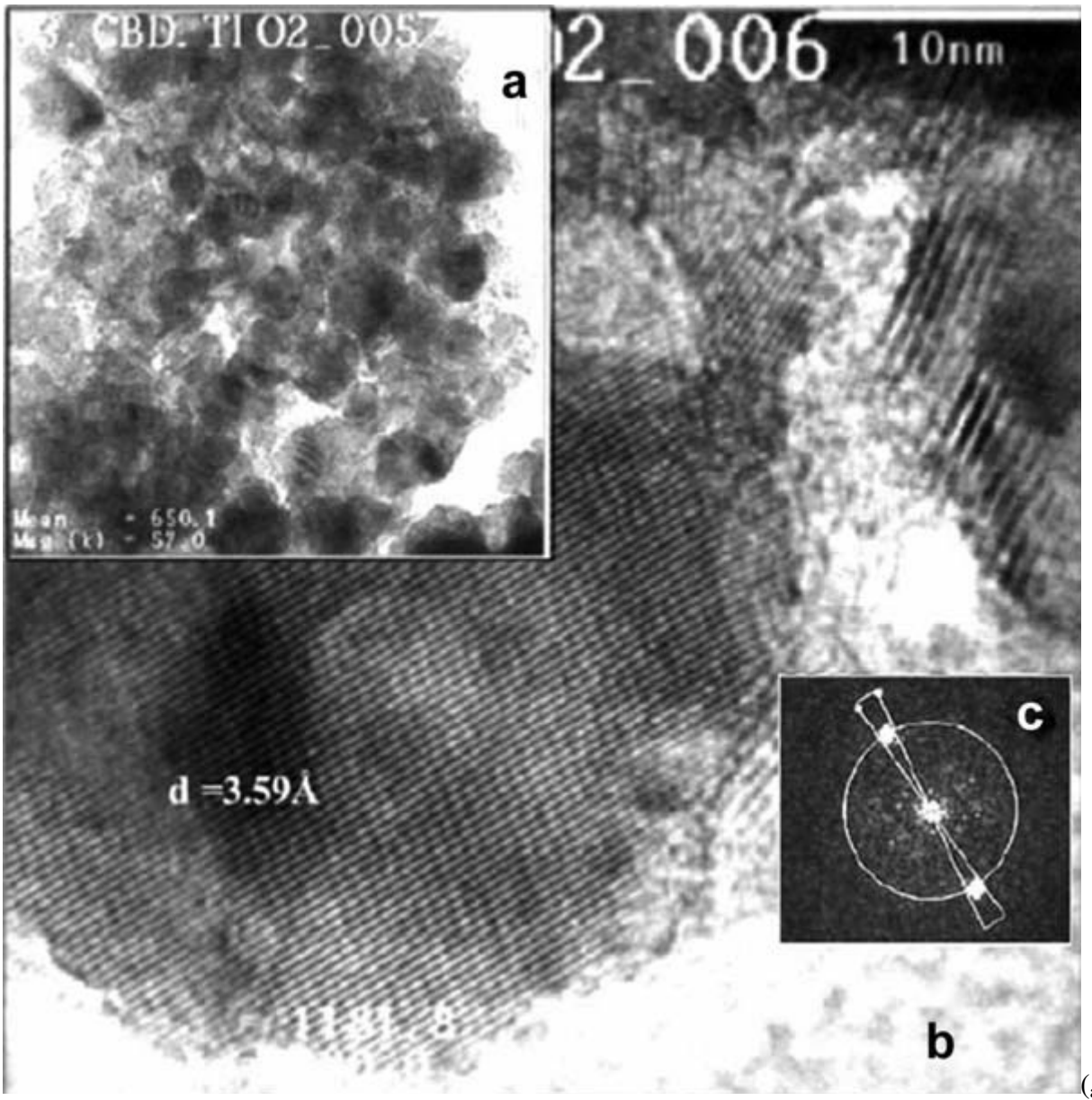

(a)

Figure 17: Inset shows TEM image of the TiO2 film deposited by chemical method followed by annealing at 500 °C for 1 h in air. (b) A high-resolution image of a portion of the investigated image in (a). Results obtained after Fourier transformation of the high-resolution image is as shown in (c)

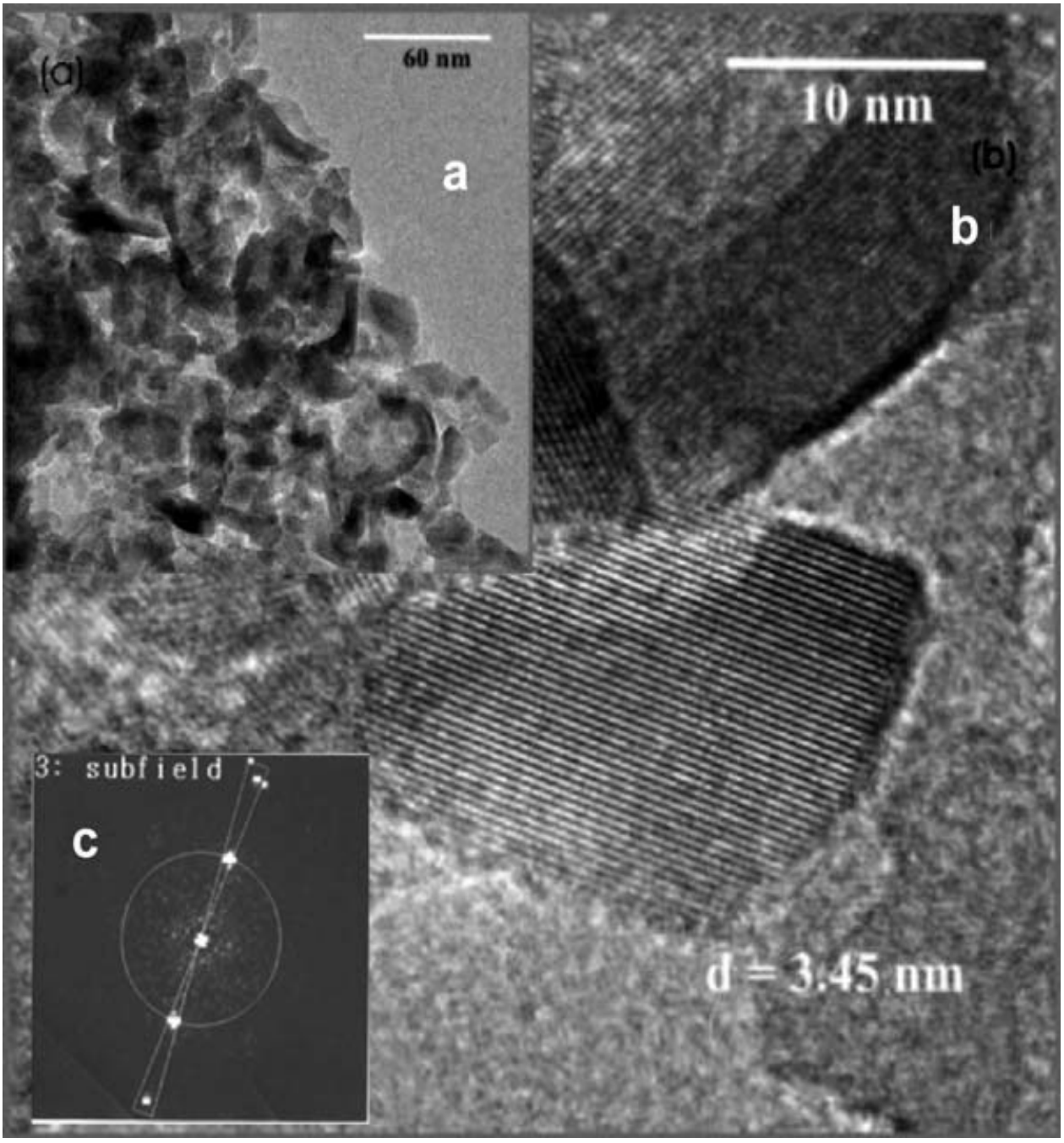

Figure18: Inset shows TEM image of the TiO2 film deposited by electrochemical method followed by annealing at 500 °C for 1 h in air. (b) A high-resolution image of a portion of the investigated image in (a). Results obtained after Fourier transformation of the high resolution image is as shown in (c).

In addition,XPS measurement was performed for electrochemically deposited films. Fig.19 shows the XPS survey spectra of the TiO2 film deposited on the ITO substrate. Major characteristic transition peaks for Ti, O and C are indicated.The 2p3/2 peak for Ti has a binding energy of 453.8 eV for metal, 455.1 for TiO, 458.5 for TiO2 while 459.2 for anatase/rutile TiO2 . The high-resolution scan (inset in Fig. 19b) showed that the photoelectron peak for Ti at 459.5 eV, which is in the form of TiO2, corresponds to anatase-phase, also supported by structural studies.

In the present case, we observed that the O1s peak was composed of two peaks revealing the presence of two forms of oxygen (inset Fig. 19c). The analysis by deconvolution shows two peaks at 530.8 and 533.2 eV. The major peak at 530.8 eV well matched with 530.1 eV for TiO2. The minor peak might be due to the oxygen from the surface contamination, which is common for eletrochemical deposited films. Also, some part of oxygen bonded with hydrogen cannot be excluded in the present case . In addition to that, contamination of the

surface by carbon is evident as peak for this element is already visible at 285.8 eV for the virgin TiO2 surface.

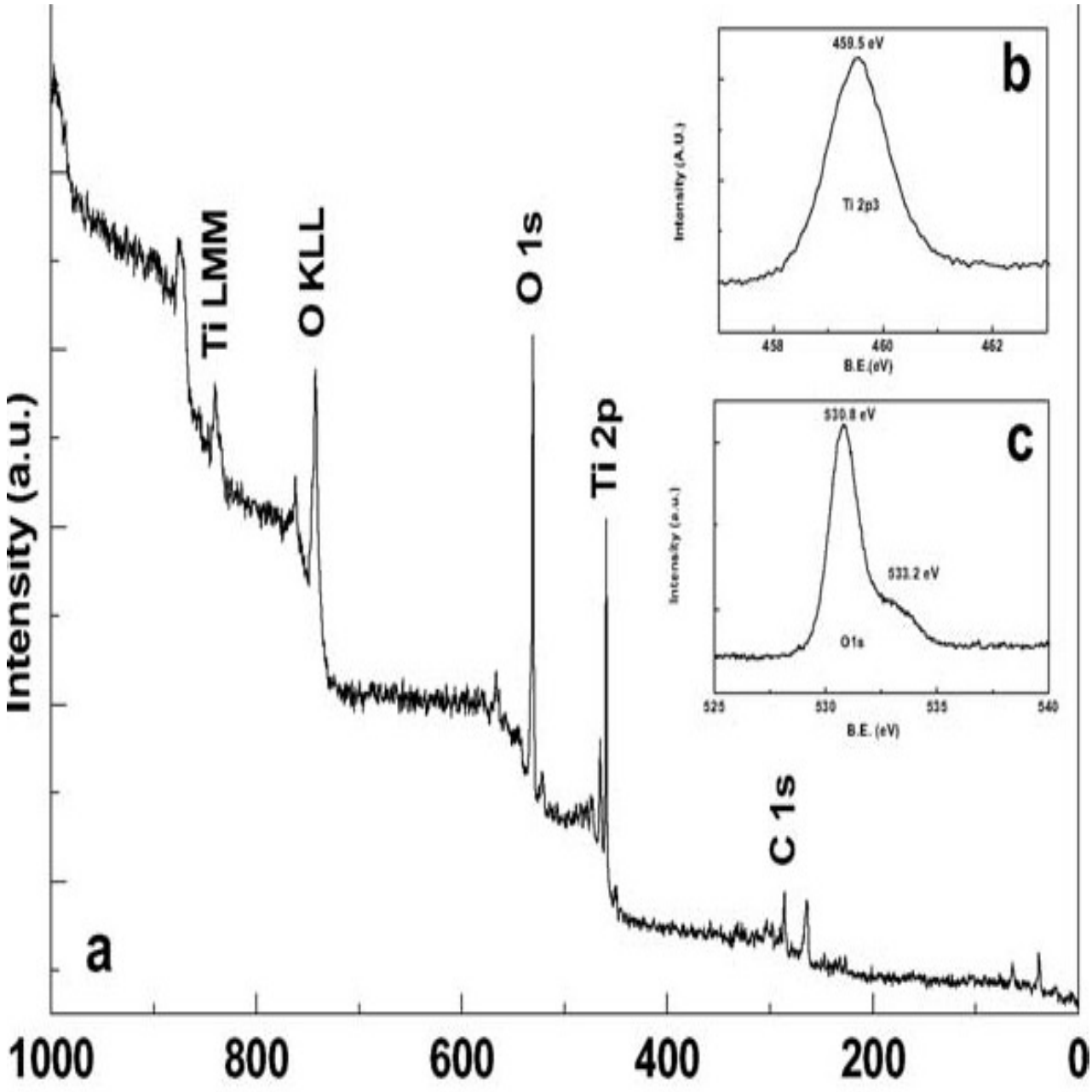

Figure19: X-ray diffraction patterns of Electrochemically deposited TiO2 thin films annealed at 500 °C for 1 h in air on (a) the glass substrate (b) the quartz substrate and (c) the collected byproduct annealed at 500 °C for 1 h in air

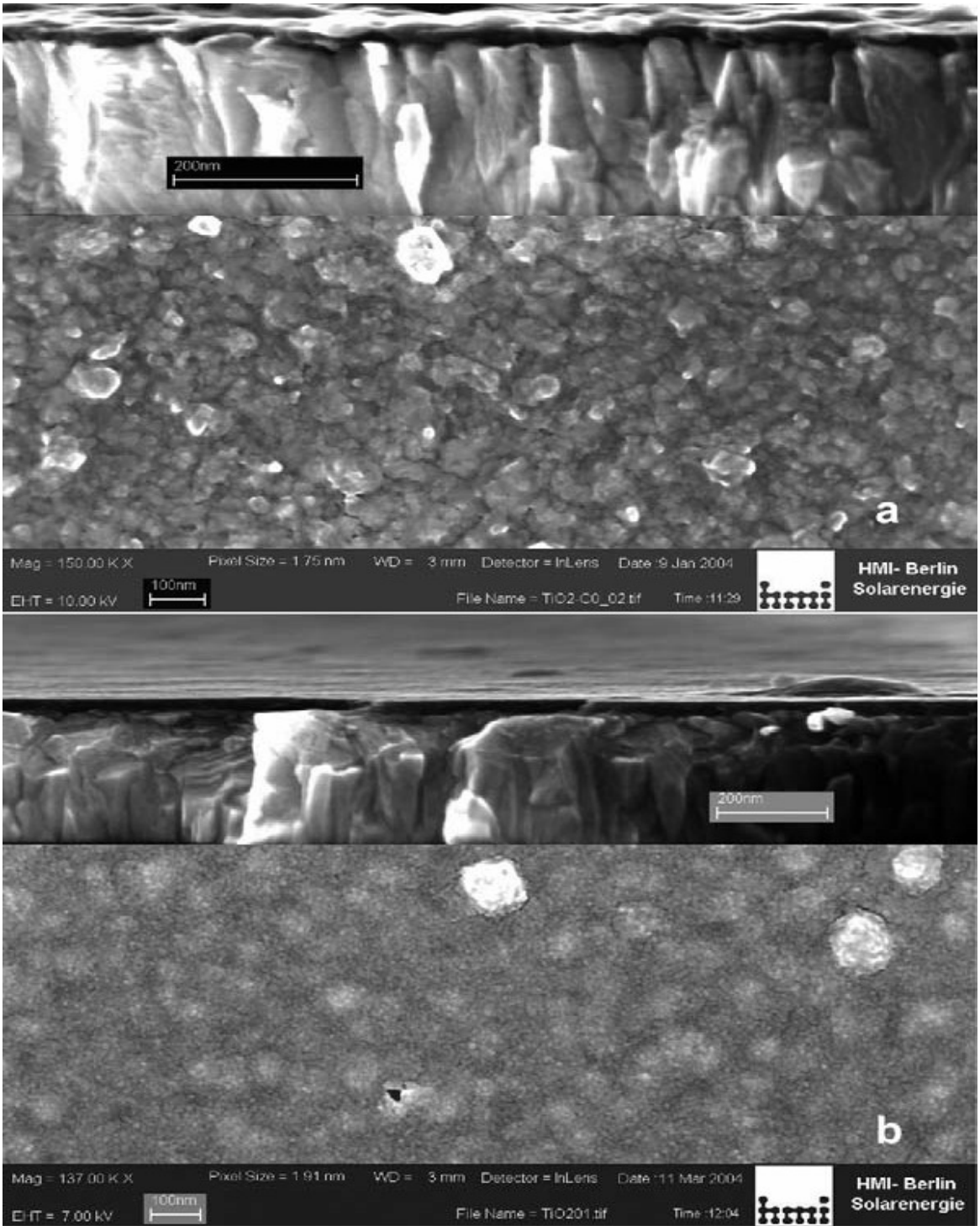

Figure 20: SEM images of the TiO2 films deposited by (a) chemical and (b) electrochemical methods followed by annealing at 500 °C for 1 h in air. Inset is the cross-section images, shows the compactness of the films.

For electrochemically deposited films, a conformal coverage of the ITO substrate without any cracks or holes was obvious. The electrodeposited film is compact with a thickness of 50 nm as

estimated by cross-sectional analysis . AFM studies in contact mode were performed for TiO2 film deposited by (a) chemical and (b) electrochemical methods on the ITO substrates (see Fig. 21). The films were dense and compact. Evaluation of surface patterns was conducted by estimating the roughness of the film (root-mean-squared). The root-meansquare (r.m.s.) roughnesses of 9 and 10 nm were evaluated from 9 μm2 surface area for chemical and electrochemical deposited films, respectively.

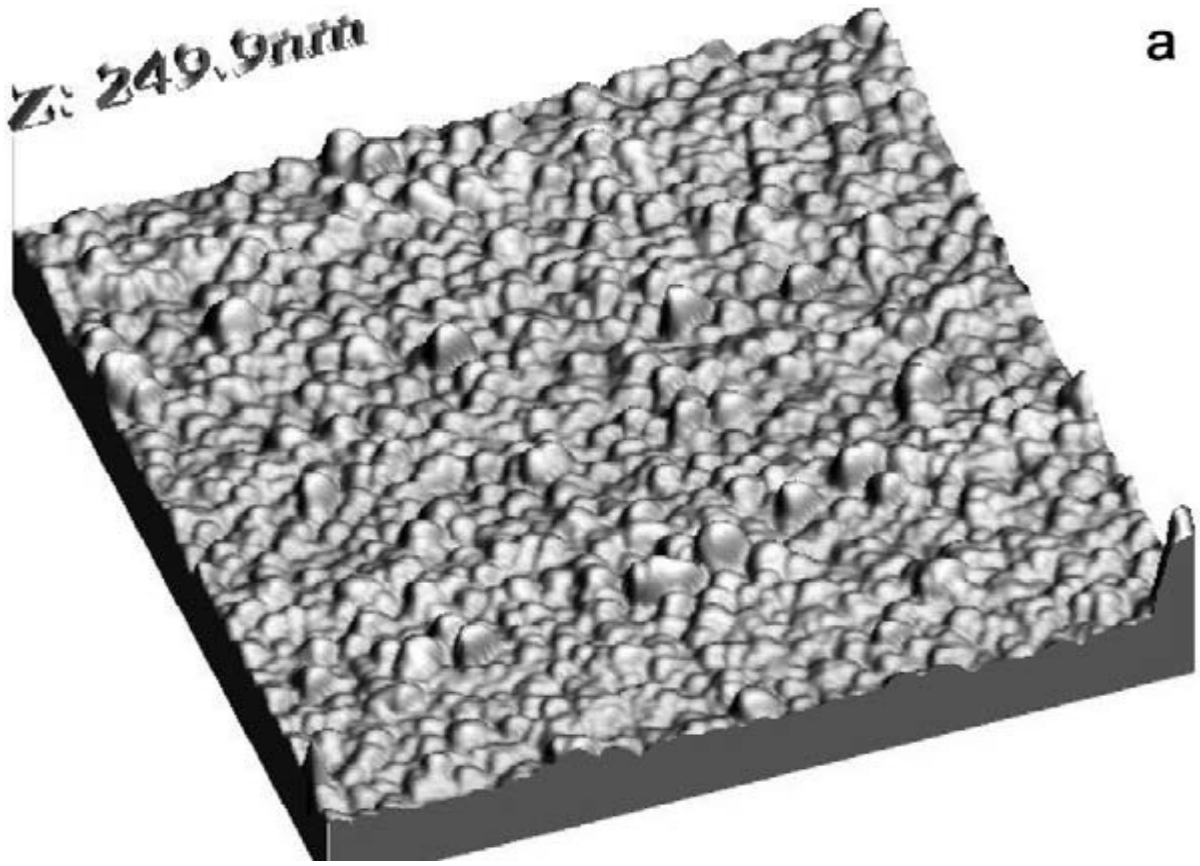

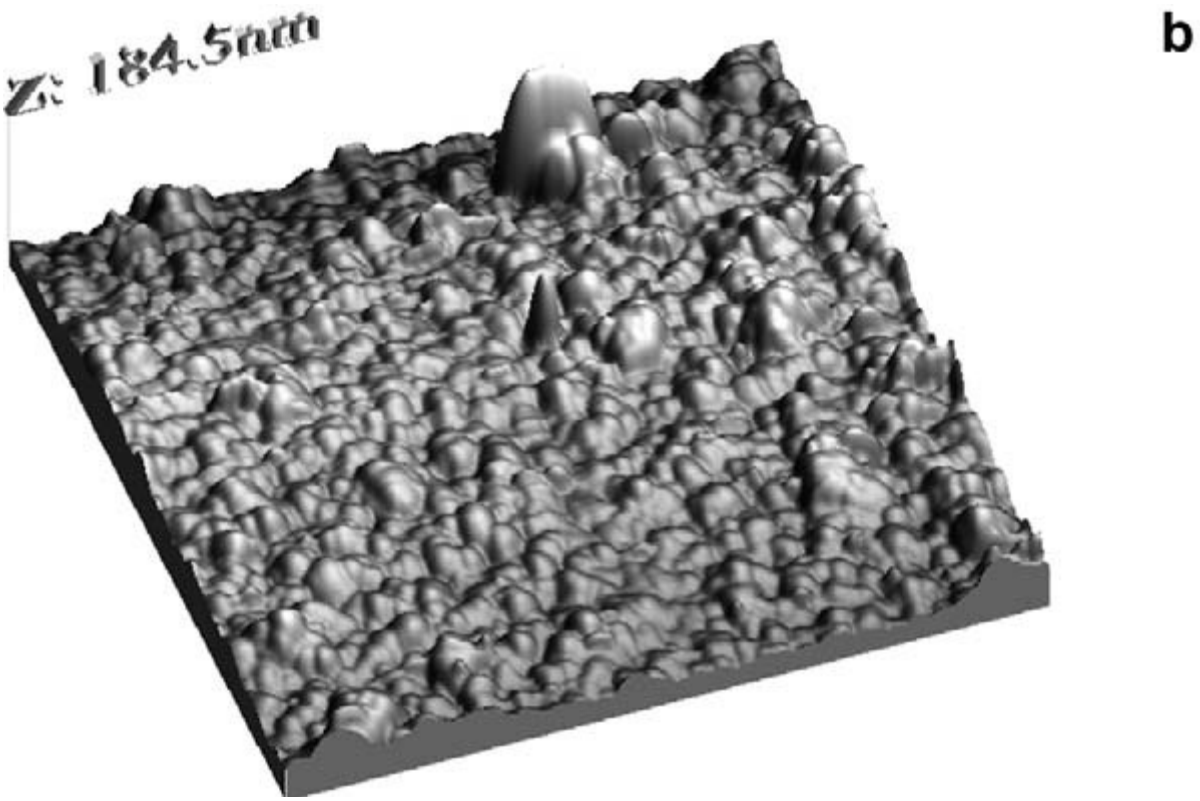

Figure 21: Surface view AFM image of the TiO2 films deposited by (a) chemical method and (b) electrochemical method followed by annealing at 500 °C for 1 h in air.

3.0. Conclusion

The Electrochemical synthesis of TMOs materials for resistive switching for ReRAM application has shown some remarkable interest in various technique in which individual TMOs material is synthesized.

In the synthesis of NiO,a one step approach is used by electrodepositing Ni and carrying out oxidation process at the state temperature.While in the case of Sn2O,synthesis is carried out in two different Oxidation process,first at a temperature lower than the melting point of Sn which helps to convert oxidize it to SnO and a higher temperature that will help to oxidize it further Sn2O.

It is of good interest to note that ZnO synthesis although uses template base synthesis do not undergo oxidation process in order to ZnO,rather it undergoes a lot of reactions ;first there is a reaction between Zinc ion and the Alumina template to form hydroxide.Then precipitation reaction of the Zinc hydroxide with the Alumina template to form ZnO by dehydration reaction.

4.0. References

[1] Int. Technology Roadmap for Semiconductors, Report on Emerging Research Devices 2011

[2] Zhuang,w.w.et al.,Tech.Dig.IEDM (2002),193

[3] Baek,I.G.,et al., Tech.Dig.IEDM (2005),750

[4] Dumas C, Deleruyelle D, Demolliens A, Muller C, Spiga S, Cianci E, Fanciulli M, Tortorelli I andBez R 2011 Resistive switching characteristics of NiO films deposited on top of W or Cu pillar bottom electrodesThin Solid Films5193798-803

[5] Choi B Jet al2005 Resistive switching mechanism of TiO2 thin films grown by atomic-layer depositionJ. Appl. Phys.98 033715

[6] Templated Assembly of Magnetic Cobalt Nanowire Arrays A.K. SRIVASTAVA, R.S. SINGH, K.E. SAMPSON,V.P. SINGH, and R.V. RAMANUJAN

[7] Lee N J, An B H, Koo A Y, Ji H M, Cho J W, Choi Y J, Kim Y K and Kang C J 2011 Resistive switching behavior in a Ni–Ag2Se–Ni nanowireApplPhys A102 897–900

[8] Tresback Jet al.2005 Engineered metal-oxide-metal heterojunction nanowires J. Mat. Res.20 10

[9] Lee N J, An B H, Koo A Y, Ji H M, Cho J W, Choi Y J, Kim Y K and Kang C J 2011 Resistive switching behavior in a Ni–Ag2Se Ni nanowireApplPhys A102 897–900

[10] Sawa A 2008 Resistive switching in transition metal oxides Materials Today11 6

[11] Waser R, Dittmann R, Staikov G and Szot K 2009 Redox-based resistive switching memories – Nanoionic mechanisms, prospects and challenges Adv. Mater.21 2632-63

[12] Seo Set al. 2005 Electrode dependence of resistance switching in polycrystalline NiO filmsAppl. Phys. Lett.87 263507

[13] Tresback Jet al.2007 Characterization and electrical properties of individual Au-NiO-Au heterojunctionnanowires IEEE Transactions on Nanotechnology6 6

[14] ZahoX et al.2008 Field-induced semiconductor-metal transition in individual NiO-Ni SchottkynanojunctionAppl. Phys. Lett.93152107

[15] Sun J L et al.2009 Metal-insulator transition in Au-NiO-Ni dual SchottkynanojunctionsNanotechnology20 455203

[16] Kim S I et al.2008 Reversible resistive switching behaviors in NiO nanowiresAppl. Phys. Lett.93033503

[17] HerderickE D et al.2009 Bipolar resistive switching in individual Au-NiO-Au segmented nanowiresAppl. Phys. Lett.95203505

[18] Song G, Chen D, Peng Z, She X, Li J and Han P 2007 Quantificational etching of AAO template

[19] J. Material Science and Technology23 427-29J. Hu, T.W. Odom, and C.M. Lieber: Chemistry and physics in one dimension: Synthesis and properties of nanowires and nanotubes. Acc. Chem. Res. 32, 435 (1999).

[20] B.R. Martin, D.J. Dermody, B.D. Reiss, M. Fang, L.A. Lyon, M.J. Natan, and T.E. Mallouk: Orthogonal self-assembly on colloidal gold-platinum nanorods. Adv. Mater. 11, 1021 (1999).

[21] Z.W. Pan, Z.R. Dai, and Z.L. Wang: Nanobelts of semiconducting oxides. Science 291, 1947 (2001).

[22] R.H. Baughman, A.A. Zakhidov, and W.A. de Neer: Carbon nanotubes—The route toward applications. Science 297, 787 (2002).

[23] Z.L. Wang: Nanowires and Nanobelts—Materials, Properties and Devices (Kluwer Academic Publishers, New York, 2003).

[24] C.M. Lieber: Nanoscale science and technology: Building big future from small things. MRS Bull. 28, 486 (2003).

[25] Y. Xia, P. Yang, Y. Sun, Y. Wu, B. Mayers, B. Gates, Y. Yin, F. Kim, and H. Yan: One-dimensional nanostructures: Synthesis, characterization, and applications. Adv. Mater. 15, 353 (2003).

[26] A. Kolmakov and M. Moskovits: Chemical sensing and catalysis by one-dimensional metal-oxide nanostructures. Ann. Rev. Mater. Sci. 34, 151 (2004).

[27] D. Al-Mawlawi, C.Z. Liu, and M. Moskovits: Nanowires formed in anodic oxide templates. J. Mater. Res. 9, 1014 (1994).

[28] H. Masuda and M. Satoh: Fabrication of gold nanodot array using anodic porous alumina as an evaporation mask. Jpn. J. App. Phys. 35, L126 (1996).

[29] J.C. Hulteen and C.R. Martin: A general template-based method for the preparation of nanomaterials. J. Mater. Chem. 7, 1075 (1997).

[30] S.R. Nicewarner-Pen˜ a, R.G. Freeman, B.D. Reiss, L. He, D.J. Peña, I.A. Dalton, R. Cromer, C.D. Keating, and M.J. Natan: Submicrometer metallic barcodes. Science 294, 137 (2001).

[31] N.I. Kovtyukhova, B.R. Martin, J.K.N. Mbindyo, P.A. Smith, B. Razavi, T.S. Mayer, and T.E. Mallouk: Layer-by-layer assembly of rectifying junctions in and on metal nanowires. J. Phys. Chem. B 105, 8762 (2001) 19.

[32] J.G. Wang, M.L. Tian, T.E. Mallouk, and M.H.W. Chan: Microstructure and interdiffusion of template-synthesized Au/Sn/Au junction nanowires. Nano Letters 4, 1313 (2004).

[33] H. Mehrer: Landolt-Bornstein numerical data and functional relationships in science and technology, Vol. 26, Diffusion in Solid Metals and Alloys (Springer-Verlag, Berlin, Germany, 1990).

[34] N. Kanani: Electroplating: Basic Principles, Processes, and Practice (Elsevier Advanced Technology, Oxford, U.K., 2005).

[35] S. Evoy: Dielectrophoretic assembly and integration of nanowire devices with functional CMOS operating circuitry. Microelectron. Eng. 75, 31 (2004).

[36] S. Hoeppener, R. Maoz, S.R. Cohen, L. Chi, H. Fuchs, and J. Sagiv: Metal nanoparticles, nanowires, and contact electrodes self-assembled on patterned monolayer templates—A bottom up chemical approach. Adv. Mater. 14, 1036 (2002).

[37] J.K.N. Mbindyo, B.D. Reiss, B.J. Martin, C.D. Keating, M.J. Natan, and T.E. Mollouk: DNA-directed assembly of gold nanowires on complementary surfaces. Adv. Mater. 13, 249 (2001).

[38] J.J. Urban, J.E. Spanier, L. Ouyang, W.S. Yun, and H. Park: Single-crystal barium titanate nanowires. Adv. Mater. 15, 423 (2003).

[39] A.P. Li, F. Muller, A. Birner, N. Kielsch, and U. Gosele: Hexagonal pore arrays with a 50–420 nm interpore distance formed by self-organization in anodic alumina. J. Appl. Phys. 84, 6023 (1998).

[40] Y. Wu, G. Cheng, K. Katsov, S.W. Sides, J. Wang, J. Tang, G.H. Fredrickson, M. Moskovits, and G.D. Stucky: Composite mesostructures by nano-confinement. Nature Mater. 3, 816 (2004).

[41] S.lijima.Nature (London), 354 (1999)

[42] X.F Daun .Y.Huang.Y.Cui.J.F.Wang, and C.M.Lieber Nature (London), 409, 66 (2001)